

Unidirectional Random Growth with Resetting

T. S. Biró*

Theory Department, H.A.S. Wigner RCP, Budapest, Hungary

Z. Nédá**

Department of Physics, Babeş-Bolyai University, Cluj-Napoca, Romania

Abstract

We review and classify stochastic processes without detailed balance condition. We obtain stationary distributions and investigate their stability in terms of generalized entropic distances beyond the Kullback-Leibler formula. A simple stochastic model with local growth rates and direct resetting to the ground state is investigated and applied to various networks, scientific citations and Facebook popularity, hadronic yields in high energy particle reactions, income and wealth distributions, biodiversity and settlement size distributions.

Keywords:

master equation, generalized entropic divergence, distributions in complex systems

1. Introduction

The challenge for physicists in taming complexity is to identify clear and simple models with possibly few ingredients and a great and rich reign of applicability. We have in mind achievements like the Ising model of magnetism [1], the Erdős–Rényi random graph model [2, 3], or the Landau Φ^4 -theory for second order phase transitions [4]. These models have their beauty and usefulness not only in describing particular physical phenomena, but also in allowing for the gain of new fundamental insights. The Ising model led us to investigate critical behavior, the Erdős–Rényi graph to abundant research on path length and other optimization problems on random networks, and the Landau theory opened the door to study in a unified framework all types of phase transitions.

Master equations describing stochastic processes belong to a similar model class with a wide range of applicability to complex systems [5]. The question of stability of stationary solutions to such equations is recently connected to fundamental questions about the notion and correct mathematical treatment of entropy and entropic divergence. Most approaches using master equations contain equally growth and loss terms, and very often detailed balance condition is tacitly assumed. In several cases the stationary solution is presented, but the convergence rate to it is not elaborated.

In this paper we attempt an in-depth study of a particular class of stochastic processes: where the growth process dominates and only a very special transition to a ground state is allowed. This restriction immediately breaks the detailed balance condition. On the other hand such processes belong to the sample space reduction types in which a growing interest can be documented recently [6]. Despite of its simplicity this approach offers a rich variety of complex behavior with corresponding probability distribution functions (PDF-s). In full agreement with the physicist's philosophy for handling complex systems the particular model we present here is based on only two dynamical ingredients: a growth rate and a reset rate.

Going beyond this special class of master equations, in a general framework for nonlinear stochastic models we prove the reduction of entropic divergence. For a power-law dependence on the probabilities we find a formula

*Corresponding author

**Contributing author

Email addresses: Biro.Tamas@wigner.mta.hu (T. S. Biró), zneda@phys.ubbcluj.ro (Z. Nédá)

generalizing the well-known Kullback–Leibler result [7]. We relate the entropy – probability relation to the entropic divergence expression by using the uniform distribution as a reference. While in the classical logarithmic formula from this comparison the Boltzmann–Gibbs–Shannon entropy arises, in a more general case the entropic divergence cannot simply be treated as relative entropy (difference of entropies). In particular for a power-law nonlinearity in the master equation we arrive at an entropic divergence formula which is proportional, but not equal to, a difference of Tsallis q -entropies. For the original presentation of Tsallis and earlier suggestions for generalized information measures see Refs. [8–12]. For nonlinearly modified Fokker–Planck equation, leading to power-law tailed q -exponential and q -Gaussian distributions, also in connection with non-Boltzmannian entropy formulas we refer to [13–17]. Entropy production according to the second law of thermodynamics also has been studied in this framework [18–20].

In the present paper common distributions are reproduced in the framework of the growth and reset model focusing on the continuous limit. A special emphasis is put on the growth rate with linear preference (Matthew principle [21]). The reset can also be due to an exponential dilution of the sample space, not necessarily describing direct transitions to the ground state. This represents a further generalization for the applicability of this model framework.

We point out that not only the direct problem of obtaining stationary PDF-s from known transition rates can be handled, but also the reverse problem of finding the correct transition rate formula from the known PDF. This is important for many practical applications. Furthermore in some applications, like networks, one can measure both transition rates and PDF-s, offering a testground for our model master equation.

Following all these theoretical elaborations we present a number of real-world applications. We mostly select those which are familiar and fashionable among the statistical physics community: networks, citation statistics, multiplicity distributions in high energy particle and heavy-ion collisions, income and wealth distributions, biodiversity and city size frequencies. Applications of different q -nonlinear dynamical models, e.g. description of vortex dynamics in type II superconductors are given in Refs. [22, 23], and will not be discussed in this review.

Besides reading all sections in the order given, one may have a first look directly starting with the applications. However, for readers interested in fundamental problems in thermodynamics and statistical physics we recommend to dive into the details in the leading sections.

Finally we have to apologize for not presenting a classical review with detailed reference to all important achievements on the field of complex systems and the entropy generalization. Our more modest intention here is to promote an elaboration on the simple idea of a view of local growth balanced with nonlocal resetting transitions.

2. Evolution Master Equations

In complex systems frequently non-exponential, mostly power-law tailed distributions emerge as stationary ones. It is particularly intriguing the case when such stationary distributions result from unbalanced, unidirectional processes [24]. This behavior is in contrast to the classical diffusion, where sizable transition probabilities are for choosing opposite directions. In this paper we mainly deal with processes when the state variable, briefly noted by a natural number n , or by its continuous counterpart, x , evolves only in one direction, limiting ourselves to Markovian processes. Such unbalanced growth processes alone do not lead to nontrivial stationary distributions, just to a simple inverse proportionality with the local transition rates. Therefore we add a special nonlocal transition possibility from any state n back to the $n = 0$ ground state.

All transition rates, w_{nm} , starting from a state m and ending in a state n are coefficients to the respective probabilities in the evolution master equation. To start simply, we assume a linear dependence and consider

$$\dot{P}_n = \sum_m [w_{nm}P_m - w_{mn}P_n]. \quad (1)$$

Here the antisymmetric structure of the right hand side ensures that $\sum_n \dot{P}_n = 0$, so this evolution equation conserves the normalization $\sum_n P_n = 1$. We emphasize at this point that we will later also consider nonlinear dependence on the P_n probabilities.

A well-known example is the classical diffusion with a drift [25–27]. In this case n can be both higher and lower than m , but only with a single unit. The transition rates are thus local,

$$w_{nm} = \mu_m \delta_{n,m+1} + \lambda_m \delta_{n,m-1}, \quad (2)$$

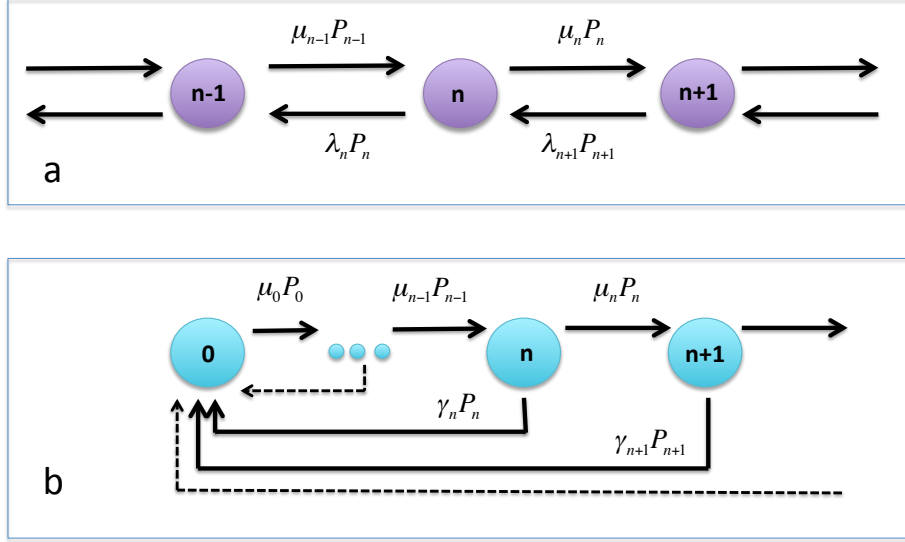


Figure 1: Markov chain for the symmetric local process with general state-dependent transition rates (top, Figure a) and for the unidirectional growth augmented by rare resets (bottom, Figure b).

leading to the evolution equation (sketched in Fig.1, top):

$$\dot{P}_n = \mu_{n-1}P_{n-1} + \lambda_{n+1}P_{n+1} - \mu_n P_n - \lambda_n P_n. \quad (3)$$

This equation is a discrete model of the one-dimensional diffusion, with position dependent drift and diffusion coefficients. In the continuous model we define the probability density function $\mathcal{P}(n\Delta x, t) = P_n/\Delta x$. The normalization is given by $\sum_n P_n = \int \mathcal{P}(x, t) dx = 1$. The drift coefficient is defined by $v(n\Delta x) = (\lambda_n - \mu_n)\Delta x$, the diffusion coefficient by $D(n\Delta x) = (\lambda_n + \mu_n)\Delta x^2/2$. This leads to the Fokker-Planck equation:

$$\frac{\partial \mathcal{P}}{\partial t} = \frac{\partial}{\partial x} (v\mathcal{P}) + \frac{\partial^2}{\partial x^2} (D\mathcal{P}). \quad (4)$$

Such systems are well-studied [28] and several theorems are known about their stationary distributions and stability, describing among others the evolution towards the stationary state.

We would like to deal here, however, with extremely different processes, typically with those when the transitions between elementary states are unidirectional, increasing n by one unit. This local growth rate is supplemented by a nonlocal transition, directly resetting any state to ground state ($n = 0$):

$$w_{nm} = \mu_m \delta_{n,m+1} + \gamma_m \delta_{n,0}. \quad (5)$$

We refer to such stochastic evolutions as "unidirectional growth with resetting". The above transition rates after summation over the starting states m lead to the following time evolution:

$$\dot{P}_n = \mu_{n-1}P_{n-1} + \delta_{n,0} \langle \gamma \rangle - (\mu_n + \gamma_n)P_n. \quad (6)$$

In the above equation $\langle \gamma \rangle = \sum_j \gamma_j P_j$ and only $n \geq 0$ is possible. The Markov chain for such systems is depicted in Fig.1 (bottom). Further simplification may arise when one specifies the step-up rates, μ_n , and the reset rates, γ_n . The simplest choice with constant transition rates, although already powerful, does not describe the most interesting phenomena. On the other hand state-dependent rates lead to several nontrivial distributions. In particular we study growth rates linear in n with constant reset rates, and discuss further possibilities, too.

3. Entropic Divergence Evolution

Entropy plays an important role in studies of convergence and stability of random processes. The purpose of this section is to find the proper expression for entropy for growth processes that do not fulfill the detailed balance condition. While studying the convergence of arbitrary initial distributions towards the stationary one, we construct the entropic distance measure which has to shrink. We derive new generalized entropy formulas based on the entropic distance tailored on a given class of dynamics.

3.1. Decreasing entropic distances for processes without detailed balance

First we have a look at linear master equations with transition rates w_{nm} which are not satisfying the detailed balance condition,

$$\frac{w_{nm}}{w_{mn}} \neq \frac{Q_n}{Q_m}. \quad (7)$$

The stochastic dynamics is described by the following linear master equation

$$\dot{P}_n = \sum_m [w_{nm} P_m - w_{mn} P_n]. \quad (8)$$

The stationary distribution by definition satisfies merely the following total balance

$$0 = \sum_m [w_{nm} Q_m - w_{mn} Q_n]. \quad (9)$$

This can be rearranged into the well known "self averaging" form:

$$Q_n = \frac{\sum_m w_{nm} Q_m}{\sum_m w_{mn}}. \quad (10)$$

We would like to construct an entropic divergence formula, represented by the real-valued functional, $\rho[P, Q]$, whose shrinking describes the approach from any actual probability distribution $P_n(t)$ towards the stationary one, Q_n . The functional $\rho[P, Q]$ has to respect the following general properties:

1. $\rho[P, Q] \geq 0$ for any pair of normalized distributions P_n and Q_n .
2. From $\rho[P, Q] = 0$ it uniquely follows that $P_n = Q_n$.
3. With Q_n being the stationary distribution it evolves according to $\dot{\rho}[P, Q] \leq 0$.
4. $\dot{\rho}[P, Q] = 0$ achieved only if $P_n = Q_n$.

We note by passing that symmetry is not necessary. We seek the entropic divergence in the special scaling trace form

$$\rho[P, Q] = \sum_n Q_n \sigma(\xi_n), \quad (11)$$

with $\xi_n = P_n/Q_n$ and $\sigma(\xi)$ a function whose properties we discuss later. This distance measure is not symmetric for the exchange of P and Q , therefore it cannot be used for extracting metric properties, like the triangle inequality in the space of possible distributions. A symmetrization, however, can be achieved by using the sum

$$\rho[P, Q] + \rho[Q, P] = \sum_n Q_n [\sigma(\xi_n) + \xi_n \sigma(1/\xi_n)]. \quad (12)$$

This is equivalent with using the core function

$$\kappa(\xi) \equiv \sigma(\xi) + \xi \sigma(1/\xi) \quad (13)$$

in each term in the sum.

The property to have non-negative entropic divergence can be related to the curvature of the core function $\sigma(\xi)$ by making use of the Jensen inequality:

$$\sum_n Q_n \sigma(\xi_n) \geq \sigma\left(\sum_n Q_n \xi_n\right) = \sigma\left(\sum_n P_n\right) = \sigma(1) \quad (14)$$

for $\sigma'' > 0$. For satisfying properties 1 and 2 one uses core functions with overall positive second derivative and $\sigma(1) = 0$. From these conditions also follows $\kappa(1) = 0$ and $\kappa'' > 0$. Studying the first and second derivative of the symmetrized distance's core function, $\kappa(\xi)$, we arrive at an interesting consequence. One easily obtains $\kappa(1) = 2\sigma(1) = 0$, $\kappa'(1) = 0$ and $\kappa'' > 0$. This means that $\xi = 1$ is the minimum of $\kappa(\xi)$ with the value zero, therefore for all ratios $\xi_n = P_n/Q_n$ we have a positive contribution to the symmetrized distance: $\kappa(\xi) \geq 0$ (cf. Fig.2).

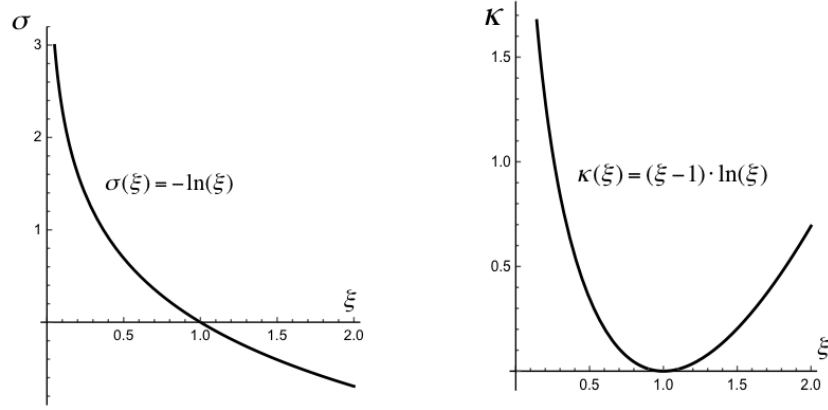


Figure 2: An example for the core functions $\sigma(\xi) = -\ln \xi$ and its $[P, Q]$ symmetrized counterpart $\kappa(\xi) = (\xi - 1) \ln \xi$.

According to the trace form (11) the time derivative of the entropic divergence from the stationary distribution, Q_n , is given as follows

$$\dot{\rho} = \sum_n \sigma'(\xi_n) \dot{P}_n = \sum_{n,m} \sigma'(\xi_n) (w_{nm} Q_m \xi_m - w_{mn} Q_n \xi_n). \quad (15)$$

Applying the identity $\xi_m = \xi_n + (\xi_m - \xi_n)$ we get

$$\dot{\rho} = \sum_n \xi_n \sigma'(\xi_n) \sum_m (w_{nm} Q_m - w_{mn} Q_n) + \sum_{n,m} \sigma'(\xi_n) (\xi_m - \xi_n) w_{nm} Q_m. \quad (16)$$

Here the first sum contains a term which is zero due to the total balance condition eq.(9). The sign of the remaining terms in the double sum depends on the factor $\sigma'(\xi_n)(\xi_m - \xi_n)$. This is the first order term in the Taylor expansion. Indeed the remainder theorem for Taylor series in the Lagrange form ensures that

$$\sigma(\xi_m) = \sigma(\xi_n) + \sigma'(\xi_n) (\xi_m - \xi_n) + \frac{1}{2} \sigma''(\xi_{mn}) (\xi_m - \xi_n)^2 \quad (17)$$

with some ξ_{mn} in the interval $[\xi_n, \xi_m]$. With this we arrive at

$$\dot{\rho} = \sum_{n,m} (\sigma(\xi_m) - \sigma(\xi_n)) w_{nm} Q_m - \frac{1}{2} \sum_{n,m} \sigma''(\xi_{mn}) (\xi_m - \xi_n)^2 w_{nm} Q_m. \quad (18)$$

The sum

$$\sum_{n,m} (\sigma(\xi_m) - \sigma(\xi_n)) w_{nm} Q_m, \quad (19)$$

vanishes due to exchanging the summation indices only in the first term:

$$\sum_{n,m} \sigma(\xi_n) (w_{mn} Q_n - w_{nm} Q_m) = 0, \quad (20)$$

because of the total balance condition. Since $\sigma'' > 0$ the sign of $\dot{\rho}$ is hereby non-positive:

$$\dot{\rho} = -\frac{1}{2} \sum_{n,m} \sigma''(\xi_{nm}) (\xi_m - \xi_n)^2 w_{nm} Q_m \leq 0. \quad (21)$$

This result teaches us that by satisfying conditions 1 and 2 by $\sigma'' > 0$ and $\sigma(1) = 0$ conditions 3 and 4 are automatically satisfied. The above sum (21) vanishes only if all $\xi_m = \xi_n$. Since both P_n and Q_n are normalized, this is only possible if $P_n = Q_n$.

Finally we present the entropic divergence formula applied for the unidirectional grow and reset dynamics using the classical ansatz $\sigma(\xi) = -\ln \xi$:

$$\dot{\rho} = -\frac{1}{2} \sum_m \frac{(\xi_m - \xi_{m+1})^2}{\xi_{m,m+1}^2} \mu_m Q_m - \frac{1}{2} \sum_m \frac{(\xi_m - \xi_0)^2}{\xi_{m,0}^2} \gamma_m Q_m. \quad (22)$$

3.2. A treatable generalization

In the previous subsection a proof by construction of a proper entropic divergence formula was given for general linear master equations without assuming the detailed balance condition for the transition rates w_{nm} . This result can easily be extended to dynamical models based on nonlinear master equations of the type

$$\dot{P}_n = \sum_m [w_{nm} a(P_m) - w_{mn} a(P_n)] \quad (23)$$

with $a(P)$ being a positive valued function. Practically one repeats the derivation discussed above, with the important difference that now $\xi = a(P)/a(Q)$ is the reference variable to be used.

The stationary distribution, Q_n , can be obtained by solving the total balance equation

$$0 = \sum_m [w_{nm} a(Q_m) - w_{mn} a(Q_n)]. \quad (24)$$

We seek for an entropic divergence in the trace form

$$\rho[P, Q] \equiv \sum_n \sigma(P_n, Q_n) \geq 0, \quad (25)$$

respecting conditions 1 and 2.

The time derivative of this entropic distance is

$$\dot{\rho} = \sum_n \frac{\partial \sigma}{\partial P_n} \cdot \dot{P}_n. \quad (26)$$

Using eq.(23) it reads as

$$\dot{\rho} = \sum_{n,m} \frac{\partial \sigma}{\partial P_n} [w_{nm} a(Q_m) \xi_m - w_{mn} a(Q_n) \xi_n]. \quad (27)$$

In the second term of the above double sum we can perform the summation over m using the total balance (24) leading to

$$\dot{\rho} = \sum_{n,m} \left[\frac{\partial \sigma}{\partial P_n} (\xi_m - \xi_n) \right] w_{nm} a(Q_m). \quad (28)$$

We also can add a term,

$$\sum_{m,n} (\lambda_n - \lambda_m) w_{nm} a(Q_m), \quad (29)$$

which is zero. We utilize the total balance eq.(24) in order to show that this term is indeed zero. The proof is based on exchanging the summation indices n and m in the subtracted second term:

$$\sum_{n,m} (\lambda_n - \lambda_m) w_{nm} a(Q_m) = \sum_n \lambda_n \sum_m [w_{nm} a(Q_m) - w_{mn} a(Q_n)] = 0. \quad (30)$$

Collecting all these results we rewrite the time derivative of the entropic divergence as

$$\dot{\rho} = \sum_{n,m} \left[\frac{\partial \sigma}{\partial P_n} (\xi_m - \xi_n) + (\lambda_n - \lambda_m) \right] w_{nm} a(Q_m). \quad (31)$$

For satisfying the second law of thermodynamics (conditions 3 and 4) one aims to attend a definite sign to $\dot{\rho}$. It is achieved by a similar construction as in the linear case. We set

$$\frac{\partial \sigma}{\partial P_n} = s'(\xi_n), \quad (32)$$

and choose $\lambda_n = s(\xi_n)$ in eq.(28). With this the factor in the square brackets becomes

$$s'(\xi_n) (\xi_m - \xi_n) + s(\xi_n) - s(\xi_m) = -\frac{1}{2} s''(\xi_{mn}) (\xi_m - \xi_n)^2, \quad (33)$$

and we can use again the remainder theorem for Taylor series in the Lagrange form. Again ξ_{mn} is a value between ξ_m and ξ_n , endpoints included. Our final result for the time derivative of the entropic divergence is then summarized as follows:

$$\dot{\rho} = -\frac{1}{2} \sum_{n,m} s''(\xi_{mn}) (\xi_m - \xi_n)^2 w_{nm} a(Q_m). \quad (34)$$

We conclude that the only requirement for $\dot{\rho} \leq 0$ is that the function $s(\xi)$ is subject to $s''(\xi) > 0$ for all arguments. Having the function $s(\xi)$ one reconstructs the entropic divergence as a sum of $\sigma(P_n, Q_n)$ terms by solving the partial differential equation

$$\frac{\partial \sigma}{\partial P_n} = s' \left(\frac{a(P_n)}{a(Q_n)} \right). \quad (35)$$

Integration constants have to be set according to $\rho[Q, Q] = 0$, i.e. $\sigma(Q_n, Q_n) = 0$. According to our best knowledge in this very general case we are the first to deliver such a proof.

3.3. An example: q -generalization of the Kullback–Leibler divergence

The classical result occurs for linear dynamical models, $a(P) = P$, if one uses $\sigma(\xi) = -\ln \xi$. The procedure described above arrives at the Kullback-Leibler divergence formula for the entropic distance.

$$\rho[P, Q] = \sum_n Q_n \ln \frac{Q_n}{P_n}. \quad (36)$$

Another example is given by the divergence using $a(P) = P^q$. In this case we have

$$\frac{\partial \sigma}{\partial P_n} = -(Q_n/P_n)^q, \quad (37)$$

and the solution of eq.(35) with the proper integration constant leads to

$$\rho[P, Q] = \frac{1}{1-q} \left(1 - \sum_n Q_n^q P_n^{1-q} \right). \quad (38)$$

This entropic divergence formula is of the special scaling trace formula

$$\rho[P, Q] = \sum_n Q_n f(P_n/Q_n), \quad (39)$$

with the special function

$$f(x) = \frac{1 - x^{1-q}}{1-q} = -\ln_q(x). \quad (40)$$

Since $f''(x) = qx^{-q-1} > 0$ for $q > 0$ the Jensen inequality ensures properties 1 and 2. In order to realize this we recall

$$\sum_n Q_n f(P_n/Q_n) \geq f\left(\sum_n Q_n \frac{P_n}{Q_n}\right) = f(1) = 0. \quad (41)$$

This means

$$\rho[P, Q] \geq 0. \quad (42)$$

Recalling the formula for the Tsallis entropy,

$$S_T[Q] = \frac{1}{q-1} \sum_n (Q_n - Q_n^q), \quad (43)$$

one obtains $S_T[U] = (W^{1-q} - 1)/(1 - q)$ for the uniform distribution. Now the entropic divergence between the stationary distribution, Q and the uniform distribution, $U_n = 1/W$ for $n = 1, 2, \dots, W$ can be expressed as

$$\rho[U, Q] = W^{q-1} \{S_T[U] - S_T[Q]\}. \quad (44)$$

Here $\rho[U, Q] \geq 0$ ensures that among all possible stationary distributions, Q_n , the uniform distribution has the maximal Tsallis entropy, i.e. $S_T[U] \geq S_T[Q]$.

This properly constructed entropic divergence is proportional to the difference of Tsallis entropies (not the Rényi ones) for comparing the uniform distribution with the stationary one. The proportionality constant, W^{q-1} , in eq.(44) can be melted with the definition of $\rho[U, Q]$. This is an argument in favor of Tsallis entropy instead of the Rényi formula.

In this subsection we have shown two examples of analytic expressions for the entropic divergence.

3.4. When detailed balance is necessary

Here we study the case when the transition probability from one state of the system to another depends on both the initial and final state occupation probabilities. Our above presented proof now fails, and only detailed balance conditioned elementary rates allow for a definite sign of the change of entropic distances. Already for a factorized dependence the detailed balance is necessary.

We consider here the dynamical equation

$$\dot{P}_n = \sum_m [w_{nm}a(P_m)b(P_n) - w_{mn}a(P_n)b(P_m)] \quad (45)$$

together with trace form quantity

$$\rho[P, Q] \equiv \sum_n \sigma(P_n, Q_n). \quad (46)$$

The change of this quantity in time is given as

$$\dot{\rho} = \sum_n \frac{\partial \sigma}{\partial P_n} \dot{P}_n. \quad (47)$$

Now we use the index antisymmetry inherent in eq.(45) to obtain

$$\dot{\rho} = \frac{1}{2} \sum_{n,m} w_{nm}a(P_m)b(P_n) \left[\frac{\partial \sigma}{\partial P_n} - \frac{\partial \sigma}{\partial P_m} \right] \cdot \left[1 - \frac{w_{mn}a(P_n)b(P_m)}{w_{nm}a(P_m)b(P_n)} \right]. \quad (48)$$

Due to the mixed dependence on n - and m -indexed quantities the monotonicity or second derivative argumentation, presented in the previous subsections, cannot be carried out now. However, assuming that the transition rates, w_{nm} and w_{mn} satisfy the *detailed balance condition* with the stationary distribution,

$$\frac{w_{mn}}{w_{nm}} = \frac{b(Q_n)a(Q_m)}{a(Q_n)b(Q_m)}, \quad (49)$$

we obtain

$$\dot{\rho} = \frac{1}{2} \sum_{n,m} w_{nm} a(P_m) b(P_n) \left[\frac{\partial \sigma}{\partial P_n} - \frac{\partial \sigma}{\partial P_m} \right] \cdot \left[1 - \frac{f(P_n)/f(Q_n)}{f(P_m)/f(Q_m)} \right] \quad (50)$$

with the general function $f(x) = a(x)/b(x)$. The above result can be rewritten in terms of the original rates as

$$\dot{\rho} = \frac{1}{2} \sum_{n,m} w_{nm} b(P_n) b(P_m) f(Q_m) \left[\frac{\partial \sigma}{\partial P_n} - \frac{\partial \sigma}{\partial P_m} \right] \cdot \left[\frac{f(P_m)}{f(Q_m)} - \frac{f(P_n)}{f(Q_n)} \right]. \quad (51)$$

From here it is obvious that one shall use the following ratio variable

$$\xi_n = \frac{f(P_n)}{f(Q_n)} = \frac{a(P_n) b(Q_n)}{a(Q_n) b(P_n)}. \quad (52)$$

For a definite sign, $\dot{\rho} \leq 0$ one needs that

$$\frac{\partial \sigma}{\partial P_n} = s'(\xi_n) \quad (53)$$

to obtain

$$[s'(\xi_n) - s'(\xi_m)] \cdot [\xi_m - \xi_n] \leq 0. \quad (54)$$

This expression, based again on the remainder theorem for Taylor series can be expressed using $s''(\xi_{nm})$ at an intermediate point. Finally we arrive at

$$\dot{\rho} = -\frac{1}{2} \sum_{n,m} w_{nm} b(P_n) b(P_m) f(Q_m) s''(\xi_{nm}) (\xi_m - \xi_n)^2. \quad (55)$$

Global stability is achieved for any $s'' > 0$ function. This is the same result as in the previous subsection eq.(34), but only subject to the detailed balance condition.

Again, if $a(P) \neq P$ and $b(P) \neq 1$, the classical choice, $s(\xi) = -\ln \xi$, does not lead to the Kullback–Leibler form in terms of the probabilities P_n and Q_n . In such cases $\xi_n \neq P_n/Q_n$. However a modified connection to the entropy formula also occurs in this general treatment. With the standard logarithmic $s(\xi)$ function one has

$$\frac{\partial \sigma}{\partial P} = -\frac{1}{\xi} = -\frac{f(Q)}{f(P)}. \quad (56)$$

Its proper solution utilizes the primitive function, $g(x) = \int \frac{dx}{f(x)}$:

$$\sigma(P, Q) = f(Q)(g(Q) - g(P)) = \frac{g(Q) - g(P)}{g'(Q)}. \quad (57)$$

Using the Taylor series remainder theorem again up to the second derivative the entropic distance equals to the following expression

$$\rho[P, Q] = -\frac{1}{2} \sum_n \frac{g''(R_n)}{g'(Q_n)} (P_n - Q_n)^2 \quad (58)$$

with $R_n \in [Q_n, P_n]$ being a certain value between P_n and Q_n . Finally using the function $f(x)$ instead of the derivatives of $g(x)$ we arrive at the expression

$$\rho[P, Q] = \frac{1}{2} \sum_n \frac{f'(R_n)}{f^2(R_n)} f(Q_n) (P_n - Q_n)^2. \quad (59)$$

This expression is positive for all dynamics using $f' > 0$ for unequal P and Q distributions and zero only if they coincide. Common choices, like $a(P) = P$, $b(P) = 1 + \lambda P$, satisfy this condition. Physical values for λ are bigger than -1 .

The distance between the uniform and the stationary distribution is given by

$$\rho[U, Q] = Z[Q] (S[U] - S[Q]) \quad (60)$$

with the entropy definition

$$S[Q] \equiv -\frac{1}{Z[Q]} \sum_n f(Q_n) g(Q_n) \quad (61)$$

and the distribution-dependent sum

$$Z[Q] \equiv \sum_n f(Q_n). \quad (62)$$

As eq.(60) clearly shows the entropic distance in this more general case cannot be interpreted as relative entropy due to the Q -dependence of the prefactor.

Finally closing this subsection we note that a non-factorizing dependence of the transition probability on the starting and final occupation probabilities does not allow for such a proof even when detailed balance is imposed.

4. Stationary Distributions

We discuss separately the discrete and the continuous state evolutions and the corresponding stationary distributions. Several well-known statistical distributions are successfully reconstructed in the framework of this unified mathematical model.

4.1. Discrete state space processes

In order to identify the stationary distributions, Q_n , one considers $\dot{P}_n = 0$ and solves the evolution equation:

$$0 = \sum_m [w_{nm} Q_m - w_{mn} Q_n]. \quad (63)$$

For unidirectional growth with resetting for any $n > 0$ we obtain a simple recursion

$$\mu_{n-1} Q_{n-1} = (\mu_n + \gamma_n) Q_n. \quad (64)$$

The $n = 0$ state has to be handled carefully. Q_0 can be obtained either from the normalization condition, $\sum_n Q_n = 1$, or using eq.(6) for $n = 0$

$$0 = \sum_{n=0}^{\infty} \gamma_n Q_n - (\mu_0 + \gamma_0) Q_0. \quad (65)$$

These alternative ways always lead to the same result. This nontrivial statement was proven for semi-infinite chains in [24]. The resolution of this recursion is finally given by

$$Q_n = \frac{\mu_0 Q_0}{\mu_n} \prod_{j=1}^n \left(1 + \frac{\gamma_j}{\mu_j}\right)^{-1}. \quad (66)$$

Let us discuss now particular transition rates. First we consider constant (initial state-independent) growth and resetting rates, $\mu_n = \mu$, $\gamma_n = \gamma$. The recursion equation (66) delivers the n -th power of the same term:

$$Q_n = Q_0 \left(1 + \frac{\gamma}{\mu}\right)^{-n}. \quad (67)$$

This is the *geometrical distribution*, which is easily transformed to an exponential,

$$Q_n = \frac{\gamma}{\mu + \gamma} e^{-n \ln(1 + \gamma/\mu)}. \quad (68)$$

In the case when n denotes the number of energy quanta, $E_n = n\epsilon$, this formula reproduces the Boltzmann distribution with the temperature

$$k_B T = \frac{\epsilon}{\ln(1 + \gamma/\mu)}. \quad (69)$$

For non-thermic applications, one can view this quantity as a generalized temperature. In several practical applications the reset rate is much smaller than the growth rate, $\gamma \ll \mu$, simplifying the above notion of the temperature:

$$k_B T \rightarrow \epsilon \frac{\mu}{\gamma}. \quad (70)$$

More exciting is to consider linear preference rates for the local transition, $\mu_n = \sigma(n+b)$. This reflects the Matthew principle: "For whosoever hath, to him shall be given,..." [21]. In our mathematical model the growth rate linear in n means that the next unit will be added sooner to those who have already more. As a result of this, in a given time they gain more than the others. A state n in this respect denotes having n units of some arbitrary goods (energy, money, network connection, past citations) and $b > 0$ is a threshold parameter. Very often $b = 1$ is chosen, setting $\mu_0 = \sigma$. The stationary distribution in this case is a ratio of n -fold products with different offsets,

$$Q_n = Q_0 \prod_{j=1}^n \frac{j-1+b}{j+b+\gamma/\sigma} = Q_0 \frac{(b)_n}{(c)_n}, \quad (71)$$

with $c = b + 1 + \gamma/\sigma$. Here we use the Pochhammer symbol, $(b)_n = b(b+1)\dots(b+n-1)$, a generalization of the factorial. (Indeed $(1)_n = n!$.) From the normalization,

$$\sum_n Q_n = Q_0 \sum_{n=0}^{\infty} \frac{(b)_n}{(c)_n} = 1, \quad (72)$$

follows the final result for the stationary distribution of processes with linear preference rates:

$$Q_n = \frac{c-1-b}{c-1} \frac{(b)_n}{(c)_n}. \quad (73)$$

This is the *Waring distribution*, and has been considered in failure processes by Irwin [29, 30]. The high- n tail of this distribution is a power-law:

$$Q_n \xrightarrow{n \rightarrow \infty} \frac{\gamma}{\gamma + \sigma b} \frac{\Gamma(c)}{\Gamma(b)} n^{-1-\gamma/\sigma}. \quad (74)$$

In particular with closely vanishing resetting rates, $\gamma \rightarrow 0$ one reconstructs from this result the *Zipf distribution* [31],

$$Q_n \sim n^{-1}. \quad (75)$$

4.2. Continuous state space

Concentrating to the large n behavior of such stationary distributions, a continuous variable limit, $n \rightarrow \infty$ while $x = n\Delta x$ kept finite, is of special interest. In this limit both the evolution equation and the determination of the stationary distribution are simpler. In order to gain a nontrivial equation for the unidirectional step-up evolution with long jumps to the zero state, one realizes that the short jump and long jump coefficients have to scale differently. We define the continuous rate functions, $\mu(x)$ and $\gamma(x)$, respectively as to satisfy

$$\mu(x) \equiv \mu(n \cdot \Delta x) = \mu_n \Delta x, \quad \text{and} \quad \gamma(x) \equiv \gamma(n \cdot \Delta x) = \gamma_n. \quad (76)$$

We arrive at a flow-like continuous state space master equation

$$\frac{\partial}{\partial t} \mathcal{P}(x, t) = -\frac{\partial}{\partial x} (\mu(x) \mathcal{P}(x, t)) - \gamma(x) \mathcal{P}(x, t). \quad (77)$$

This equation essentially differs from the Fokker-Planck equation (4): the reset process leads to a genuinely new term.

The stationary probability density function (PDF) in this case is given by

$$Q(x) = \frac{\mu(0) Q(0)}{\mu(x)} e^{-\int_0^x \frac{\gamma(u)}{\mu(u)} du}. \quad (78)$$

Here $Q(0)$ is obtained from the condition $\int_0^{\infty} Q(x) dx = 1$.

We consider again simple rates, starting with $\gamma(x) = \gamma$, a state independent resetting rate. For constant growth rate, $\mu(x) = \mu$, we regain the *exponential distribution* (68) in the $\gamma_n \ll \mu_n$ limit:

$$Q(x) = \frac{\gamma}{\mu} e^{-\frac{\gamma}{\mu} x}. \quad (79)$$

For a linear preference in the growth rate, $\mu(x) = \sigma(x + b)$, the stationary PDF is the *Tsallis–Pareto distribution*,

$$Q(x) = \frac{\gamma}{\sigma b} \left(1 + \frac{x}{b}\right)^{-1-\gamma/\sigma}. \quad (80)$$

In this view the Tsallis–Pareto distribution is the continuous limit of the Waring distribution. The growth preference can also be a nonlinear function. Modelling human mortality an exponentially increasing rate has been considered by Benjamin Gompertz [32, 33]. For $\mu(x) = \sigma e^{bx}$ eq.(78) delivers the *Gompertz distribution*:

$$Q(x) = \frac{\gamma/\sigma}{1 - e^{-\gamma/b\sigma}} e^{-bx - \frac{\gamma}{b\sigma}(1 - e^{-bx})}. \quad (81)$$

Indeed the structure of the stationary PDF, suggested by eq.(78), for constant resetting rate, $\gamma(x) = \gamma$, fits in the general scheme used in modeling failure processes related to technical and health insurance studies [34, 35]. For constant γ the structure of the stationary PDF is always of the form

$$Q(x) = \frac{h(x) e^{-H(x)}}{e^{-H(0)} - e^{-H(\infty)}}, \quad (82)$$

with $h(x) = H'(x)$ being the hazard rate and $H(x)$ itself the cumulative hazard. The survival rate can be expressed by the decreasing exponential of the cumulative hazard:

$$R(x) = \int_x^{\infty} Q(u) du = \frac{e^{-H(x)} - e^{-H(\infty)}}{e^{-H(0)} - e^{-H(\infty)}}. \quad (83)$$

In the special case $H(0) = 0$ and $H(\infty) = \infty$ one arrives at $R(x) = \exp(-H(x))$. The growth rate and the constant resetting rate are related by the hazard rate

$$\mu(x) h(x) = \gamma. \quad (84)$$

4.3. Generalized fluctuation–dissipation relation

Abandoning the constancy of the resetting rate, a state dependent $\gamma(x)$ and γ_n scenario should be envisioned. Is there some compact relation between μ and γ also in this case? The answer is affirmative: from the formula (78) for the stationary PDF it is straightforward to derive that the growth rate is in general equal to a truncated expectation value of the resetting rate at stationarity:

$$\mu(x) = \frac{1}{Q(x)} \int_x^{\infty} \gamma(u) Q(u) du. \quad (85)$$

This result resembles the generalization of the fluctuation–dissipation relation, obtained by investigating a colored noise Langevin equation [37–40].

In order to support the above statement we briefly present here the main idea. In that model the Langevin equation,

$$\dot{p} + (gp - \xi) = 0, \quad (86)$$

for the momentum p of a particle moving on a line is supported by two stochastic coefficients: ξ represents the noisy pushing force while the g damping coefficient also contains a stochastic part. Altogether the average total force factor depends on the particles' momentum, p : $\langle gp - \xi \rangle = \gamma(p)$ and the Markovian (short-time) self-correlation of the noisy force contains another p -dependence

$$\langle (gp - \xi)(t)(gp - \xi)(t') \rangle = \delta(t - t') \mu(p). \quad (87)$$

The corresponding Fokker–Planck equation then includes these p -dependent (colored) noise functions:

$$\frac{\partial}{\partial t} \mathcal{P} = \frac{\partial}{\partial p} (\gamma(p)\mathcal{P}) + \frac{\partial^2}{\partial p^2} (\mu(p)\mathcal{P}). \quad (88)$$

The resulting stationary distribution is in a similar form than eq.(78),

$$Q(p) = \frac{\text{const.}}{\mu(p)} e^{-\int_0^p \frac{\gamma(u)}{\mu(u)} du}. \quad (89)$$

The fluctuation–dissipation relation becomes (85).

In the followings we turn our attention to some specific cases. For the exponential distribution $Q(x) \sim \exp(-x/T)$ combined with a constant $\gamma(x) = \gamma$ one arrives at

$$\mu(x) = T \gamma, \quad (90)$$

resembling the classical Einstein–Kubo formula.

Finally we present the discrete version of this generalized fluctuation–dissipation relation. This is easy to derive by summing up eq.(64) from the index $n + 1$ to infinity,

$$\mu_n = \frac{1}{Q_n} \sum_{m=n+1}^{\infty} \gamma_m Q_m. \quad (91)$$

For the exponential distribution, $Q_n = e^{-\beta n \epsilon} / Z$, and constant resetting rate, $\gamma_n = \gamma$, one obtains the quantum Kubo formula

$$\mu_n = \frac{\gamma}{e^{\beta \epsilon} - 1}. \quad (92)$$

Before closing this subsection we summarize the resetting and growth rates leading to the most commonly observed stationary PDF-s (Table1).

4.4. Evolution towards the stationary value

The time evolution starting from a generic initial distribution, $P_n(0)$, can be very complicated. It is more transparent to study the evolution of the ratio of continuous PDF-s to their stationary counterparts. We define

$$\xi(x, t) = \frac{\mathcal{P}(x, t)}{Q(x)}. \quad (93)$$

Substituting $\mathcal{P} = \xi Q$ into eq.(77) one obtains

$$Q \frac{\partial \xi}{\partial t} = -\xi \frac{\partial}{\partial x} (\mu Q) - \mu Q \frac{\partial \xi}{\partial x} - \gamma \xi Q. \quad (94)$$

Using the stationarity condition (78) the first and third term on the right hand side of this equation cancel each other. The remaining equation can be divided by $Q(x)$ for all x where $Q(x) \neq 0$. This results in

$$\frac{\partial \xi}{\partial t} + \mu(x) \frac{\partial \xi}{\partial x} = 0. \quad (95)$$

$\gamma(x)$	$\mu(x)$	$Q(x)$
γ	μ	Exponential: $\sim e^{-(\gamma/\mu)x}$
γ	$\sigma(x+b)$	Tsallis–Pareto: $\sim (1+x/b)^{-1-\gamma/\sigma}$
γ	$\sigma x^\alpha, \alpha < 1$	Weibull: $\sim x^{-\alpha} e^{-bx^{1-\alpha}}$
γ	$\sigma(x+a)(x+b)$	Pearson: $\sim (x+a)^{-1-\nu}(x+b)^{-1+\nu}$
γ	σe^x	Gompertz: $\sim \exp\left(\frac{\gamma}{\sigma} e^{-x} - x\right)$
$\ln(x/a)$	σx	Log-Normal: $Q(x) dx \sim e^{-\gamma^2/2\sigma} d\gamma$
x	σ^2	Gauss: $\sim e^{-x^2/2\sigma^2}$
$\sigma(ax-c)$	σx	Gamma: $\sim x^{c-1} e^{-ax}$

Table 1: Resetting and growth rates for the most common stationary PDF-s.

The above equation describes a flow with the velocity field $\mu(x)$. The evolution of the local ratio of the actual to the stationary PDF is independent of the resetting rate, $\gamma(x)$. The resetting rate was important in shaping the stationary PDF, $Q(x)$, but it plays no direct role in the evolution of this ratio. Furthermore, the time evolution of $\xi(x, t)$ is soliton-like. We consider the ξ -flow in the form

$$\frac{\partial \xi}{\partial t} = -\mu(x) \frac{\partial \xi}{\partial x} = -\frac{\partial \xi}{\partial y}, \quad (96)$$

with

$$y(x) \equiv \int_0^x \frac{du}{\mu(u)}. \quad (97)$$

The solution for ξ is a function that depends only on $y - t$, describing a general solitary wave propagating along x as driven by $\mu(x)$:

$$\xi(x, t) = f(y(x) - t) = \xi(x_t, 0) \quad (98)$$

with $dx_t/dt = -\mu(x_t)$ defining characteristic trajectories. For constant $\mu(x) = \mu$ one has $\xi(x, t) = \xi(x - \mu t, 0)$ a shift with constant velocity. With the natural boundary condition setting $\xi(0^-, t) = 1$, the deviation from the stationary PDF moves with constant velocity towards higher x . For growth rates with linear preference, $\mu(x) = \sigma(x+b)$, we obtain:

$$\xi(x, t) = \xi(xe^{-\sigma t} - b(1 - e^{-\sigma t}), 0). \quad (99)$$

In this case the deviation wave travels with an accelerating pace.

The lesson learned from this subsection is that the approach to the stationary PDF is independent of the resetting rate. We have given a compact equation with soliton-like solution for this evolution.

Instead of discussing more examples we turn in the next section to the problem of stability for the stationary PDF-s. We are particularly interested in a control quantity, called entropic divergence, between the actual $P_n(t)$ and the stationary Q_n , that can only shrink during the evolution.

4.5. Entropic divergence for the growth and resetting process

Finally, before turning to applications in complex systems, let us briefly discuss some specialties of the entropic divergence measure for the unidirectional growth and reset process.

Now we use a symmetrized entropic distance measure, $\kappa(\xi)$, for the growth and reset dynamics. Since the ratio $\xi(x, t) = \mathcal{P}(x, t)/Q(x)$, is always positive, $\kappa(\xi)$ is non-negative. The continuous entropic divergence is defined by the

following integral

$$\rho[\mathcal{P}, \mathcal{Q}] = \int_0^{\infty} \kappa(\xi(x, t)) \mathcal{Q}(x) dx \geq 0. \quad (100)$$

It evolves according to the evolution of $\xi(x, t)$. From eq.(95) it follows that

$$\frac{\partial \kappa}{\partial t} = -\mu(x) \frac{\partial \kappa}{\partial x}. \quad (101)$$

Using this equality the time derivative of the entropic distance is given by

$$\dot{\rho} = \int_0^{\infty} \frac{\partial \kappa}{\partial t} \mathcal{Q}(x) dx = - \int_0^{\infty} \mu(x) \mathcal{Q}(x) \frac{\partial \kappa}{\partial x} dx. \quad (102)$$

Partial integration by x , taking $\xi(0, t) = 1$ and therefore $\kappa(\xi(0, t)) = 0$ leads to

$$\dot{\rho} = \int_0^{\infty} \kappa(\xi(x, t)) \frac{\partial}{\partial x} (\mu(x) \mathcal{Q}(x)) dx. \quad (103)$$

Finally using the stationary solution eq.(78), we arrive at an expression which ensures the shrinking of the entropic distance to the stationary PDF for $\gamma(x) > 0$:

$$\dot{\rho} = - \int_0^{\infty} \kappa(\xi(x, t)) \gamma(x) \mathcal{Q}(x) dx \leq 0. \quad (104)$$

What is left to be proven is that this distance actually shrinks as long as the stationary PDF is achieved. For this purpose we use again the Jensen inequality,

$$\int p(x) \kappa(\xi(x, t)) dx \geq \kappa \left(\int p(x) \xi(x) dx \right), \quad (105)$$

for $\kappa'' > 0$, with an arbitrary PDF, $p(x) \in [0, 1]$, normalized as $\int_0^{\infty} p(x) dx = 1$. We choose for our purpose the following "escort type" probability density

$$p(x, t) = \frac{\gamma(x) \mathcal{Q}(x)}{\int_0^{\infty} \gamma(u) \mathcal{Q}(u) du}. \quad (106)$$

This construction results in the following bound on the shrinking rate of the symmetrized entropic distance

$$\dot{\rho} \leq -\langle \gamma \rangle_{\infty} \kappa \left(\frac{\langle \gamma \rangle_t}{\langle \gamma \rangle_{\infty}} \right). \quad (107)$$

Here we utilized the notation

$$\langle \gamma \rangle_t \equiv \int_0^{\infty} \gamma(u) \mathcal{P}(u, t) du, \quad (108)$$

and

$$\langle \gamma \rangle_{\infty} \equiv \int_0^{\infty} \gamma(u) \mathcal{Q}(u) du, \quad (109)$$

From this result it is straightforward to see that $\dot{\rho} < 0$ until the stationary PDF is achieved. At this instant $\dot{\rho} = 0$ due to $\kappa(1) = 0$.

5. Applications

In this section we review a few applications of the unidirectional sustained random growth process, described in eqs.(6) and (77). Although the data we analyze usually represent discrete distributions, for the sake of simplicity we discuss them in the continuous model's framework. The stationary distributions in the continuous limit, $Q(x)$, are of simpler form.

This type of stochastic dynamics, together with its stationary distribution, is not uncommon: very often a quantity x changes by a small amount in one step, and only in the growth direction. The low probability resetting event to the reference state $x = 0$ makes such processes nontrivial, leading to a rich variety of stationary distributions at the end.

In many systems the resetting is realized by an exponential dilatation of the sample space. Let the non-normalized density for the observed quantity, $w(x, t)$, grow in time as

$$\frac{\partial w}{\partial t} = -\frac{\partial}{\partial x}(\mu w). \quad (110)$$

This is obviously a one-directional flow. We are interested in the normalized probability density,

$$\mathcal{P}(x, t) \equiv \frac{1}{Z} w(x, t) \quad (111)$$

with

$$Z = \int_0^{\infty} w(x, t) dx. \quad (112)$$

The corresponding evolution equation for the PDF writes as

$$\frac{\partial}{\partial t} \mathcal{P}(x, t) = -\frac{\partial}{\partial x}(\mu(x) \mathcal{P}(x, t)) - \frac{\dot{Z}}{Z} \mathcal{P}(x, t). \quad (113)$$

Comparing with eq.(77) we obtain the gamma factor

$$\gamma = \frac{\dot{Z}}{Z} \quad (114)$$

which for exponentially growing systems is a constant. Therefore the results derived in section 4.2 can be directly applied.

This type of sustained random growth can be made equivalent to the sampling space reduction process family, cf. [6], based on a correspondence between transition rates leading to the same stationary distribution [41].

Our list of examples identifies the physical meaning of state labels n in the data and x in the continuous model, the elementary transition rates, γ and $\mu(x)$, and then compares the stationary distribution classified above with findings in simulations and measurements from the literature. By our restricted set of examples we are not aiming at completeness. By the richness of literature and examples of power-law tailed and other semi-exotic statistics it would be an impossible mission.

5.1. Degree distribution in networks

Our first example is already a classical one: the degree distribution, the number of connections from and to a node, in many large networks shows a stretched exponential tailed statistics. It includes the pure exponential and the power-law tails [42] as particular cases. Seemingly this is true both for directed and undirected networks [43]. In the following we speculate on how such distributions could follow from our general master equation presented above.

The simplest growth model for a network is characterized by a constant growth rate μ and a constant resetting rate γ . This leads to an exponential degree distribution at stationarity. Such distributions have been observed in world-wide marine transportation networks, in e-mail networks, power grid networks and educational collaboration networks [44]. For these complex networks the evolution dynamics does not seem to show any preference. We exemplify this simple case first by the degree distribution for the ERASMUS collaboration network of European universities studied by us earlier [49], which shows a clear exponential tail. In order to illustrate this in the left panel of Fig.3 we plot $1 - \Omega(n)$,

with $\Omega(n)$ the cumulative distribution function: $\Omega(n) = \int_0^n \rho(x)dx$. The exponential nature of this, suggests that $\rho(n)$ is also exponential. The degree distribution of this network was constructed from an exhaustive dataset available for the year 2003, containing 2333 universities and 134330 student mobilities. Two universities are connected in the network, if there has been a student exchange among them. The number of Erasmus agreements a university possesses are increasing in time. If one assumes a constant growth rate μ for this growth and an exponential increase in the number of Universities, the exponential degree distribution results from our model.

The same exponential tail is observed for the Hungarian talent-supporting organizations collaboration network [50] in the in-degree distribution. We illustrate the $\rho(n)$ dependence obtained from a logarithmically binned histogram on the right panel of Fig. 3. In 2014 there were recorded 1045 talent supporting organizations in Hungary, and with an online survey the central bureau mapped their collaboration network [51]. In the online questionnaire one had to indicate those networks with whom they had common activities. In total 4691 such directed links were revealed leading to a directed network. The number of registered talent supporting organizations is on the other hand growing fast as a function of time. Although there is no experimental evidence that this growth is exponential, one might assume such a growth for the years preceding this survey. One can speculate thus that the exponential nature of the in-degree distribution of this network can be explained with the same growth and dilution mechanism that has been discussed for the Erasmus collaboration network.

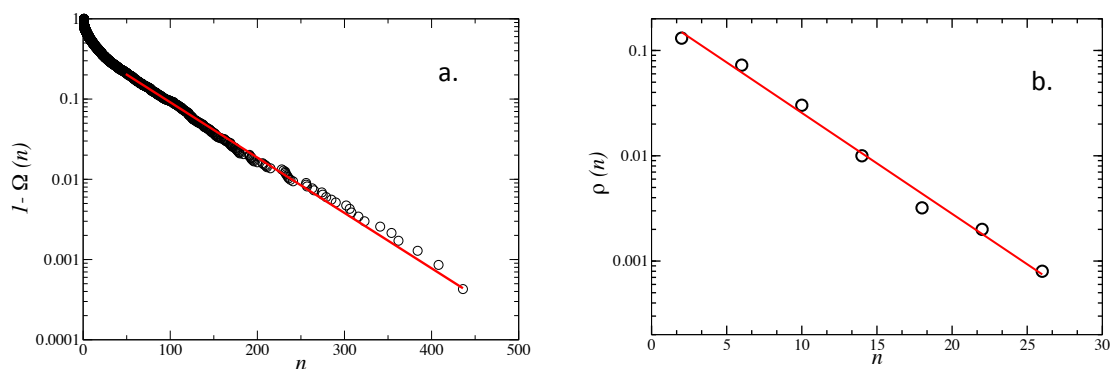


Figure 3: Exponential degree distributions in educational networks. The left figure shows results for the cumulative distribution function $1 - \Omega(k)$ for the ERASMUS student exchange networks. The right panel shows results for the logarithmically binned $\rho(k)$ in-degree distribution function for the collaboration network of the Hungarian Talent Supporting Organizations.

Preferential attachment dynamics in complex networks has also been considered. It is natural to denote the number of connections to a given node by n and then to assume a *linear preference* principle for adding the next node and its connections. In this scenario, in the growth phase of networks, the transition rate going from n to $n + 1$ connections is a linear function: $\mu_n = \sigma(n + b)$. Here very often $b = 1$ is considered. This picture has been extended to several phenomena showing network-like behavior, not only to physically linked networks. E.g. cluster size growth shows a very similar dynamics [45].

It is seldom paid attention, however, to the resetting rate. This may stem either from a dilution of the sampling space or from real resetting processes, when nodes disappear from the network. We postulate here $\gamma_n = \gamma$ as a constant rate for the long jump from having n connections to none. When random failure of nodes happens "democratically", then the rate γ_n indeed must be independent of n . Popular nodes and unimportant nodes would be diminished by the same rate in this scenario. This is in contrast to conscious attacks against a network [46], where nodes with many connections are preferred targets.

In the following discussion we restrict ourselves to the large n limit, investigating continuous distributions. The linear preference rate, $\mu(x) = \sigma(x + b)$, and a constant resetting rate, $\gamma(x) = \gamma$, determine the Tsallis–Pareto form for the stationary distribution:

$$Q(x) \sim (1 + x/b)^{-1-\gamma/\sigma}. \quad (115)$$

Indeed in Ref.[47] this degree distribution, called q -exponential, fits simulation data nicely. In [43] one finds many more examples for degree distributions exhibiting power-law type tails. The linear preference in the attachment

rate has been measured on the dynamics of internet topology, scientific collaboration and movie actor collaboration networks [48]. The authors found a preference rate nearly linear: $\mu(x) \sim x^{1.05 \pm 0.1}$ for the internet dynamics and $\mu(x) \sim x^{0.95 \pm 0.1}$ for citation networks. On the other hand the scientific co-authorship and the movie actor collaboration network shows a sublinear behavior, $\mu(x) \sim x^{0.80 \pm 0.1}$.

To exemplify the presence of a scale-free tail in systems where the dynamics is governed by a linear preferential growth, we consider the topology of the Internet on router level and use the results obtained by Mounir Affi in his master dissertation [52]. He used the data provided by the Centre for Applied Internet Data Analysis (CAIDA) [53]. The datasets contain "Traceroute" measurements conducted from CAIDA monitors, involved in the Archipelago project. Most of the data comes from monitors located in the Netherlands and Switzerland, which were supplemented with data from monitors in Spain, Germany, Finland, and Sweden. Using this data and locating the routers after their IP addresses we constructed a map of the Internet topology in a restricted area of Europe (left panel in Figure 4). The topology of the Internet wiring is illustrated in the middle panel of Figure 4. The degree distribution derived from this graph can be well fitted by the Tsallis-Pareto distribution [eq. (115)] with $b = 2.3$ and $\gamma/\sigma = 1.3$. This is illustrated in the right panel of Figure 4.

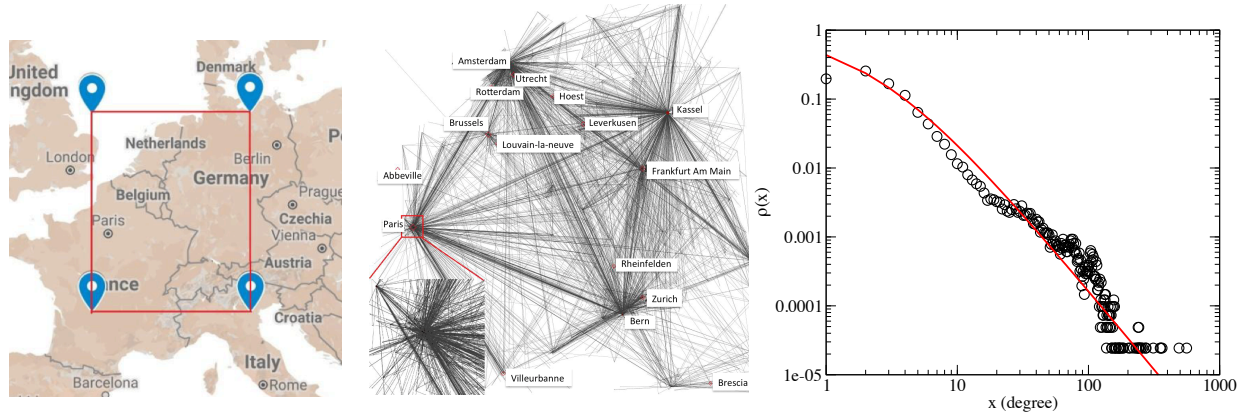


Figure 4: Results for the Internet wiring topology on router level. The left panel illustrates the mapped area of Europe. The panel in the middle sketches the unveiled wiring topology. The right panel shows the derived degree distribution (empty circles), with a Tsallis-Pareto fit [equation (115)] using $b = 2.3$ and $\gamma/\sigma = 1.3$. Figures replotted from [52] with the permission of the author.

We have briefly reviewed here the two most frequent degree distributions found in complex networks. Definitely one may find even further fits or regressions under various constraints. However, it shall be a deeper level of model making when one associates growth and resets rates to explain the degree distributions found experimentally. Finally, we have to mention here that master equations were used for modelling small-world and scale-free network topologies also in Refs. [54–56]

5.2. Distribution of citations

In a recent study concerning the statistics of citations to scientific works and shares of Facebook posts [57] we investigated such a growth model. Denoting the number of n times cited papers or Facebook posts at time t by $N_n(t)$, we allow for a preferential rate μ_n , for adding one new citation. Then the dynamics is described by the chain

$$\dot{N}_n = \mu_{n-1}N_{n-1} - \mu_n N_n \quad (116)$$

for all bins $n \geq 1$, while the number of zero cited (fresh new or never cited) articles and posts come with an increasing rate

$$\dot{N}_0 = \gamma N(t) - \mu_0 N_0, \quad (117)$$

with $N(t)$ being the total number of papers published until that time

$$N(t) \equiv \sum_{n=0}^{\infty} N_n(t). \quad (118)$$

This leads to an exponential dilution of the background:

$$\dot{N} = \sum_{n=0}^{\infty} \dot{N}_n = \gamma N, \quad (119)$$

resulting in $N(t) \sim e^{\gamma t}$. Several examples indicate that the total number of publications and Facebook posts indeed grows exponentially [57]. The corresponding equation for the fraction of n -times cited posts, $P_n(t) \equiv N_n(t)/N$, in this case is equivalent to eq.(6).

The total number of citations is given by the sum

$$C(t) \equiv \sum_{n=0}^{\infty} n N_n(t). \quad (120)$$

Its time derivative, using the above definitions, becomes

$$\dot{C} = \sum_{n=0}^{\infty} n \dot{N}_n = \sum_{n=0}^{\infty} \mu_n N_n. \quad (121)$$

Assuming again a linear preference rate

$$\mu_n = \sigma(n + b), \quad (122)$$

we get the following dynamics of the total number of citations:

$$\dot{C} = \sigma(C + bN). \quad (123)$$

The solution is given by

$$C(t) = C_0 e^{\sigma t} + \frac{\sigma b}{\gamma - \sigma} N_0 (e^{\gamma t} - e^{\sigma t}). \quad (124)$$

The average citation per post behaves as:

$$m(t) = \frac{C(t)}{N(t)} = \frac{C_0}{N_0} e^{(\sigma-\gamma)t} + \frac{\sigma b}{\gamma - \sigma} (1 - e^{(\sigma-\gamma)t}). \quad (125)$$

In realistic cases, like PubMed, Web of Science database and some popular Facebook posts (NASA, New York Times, Ronaldo) one has $\gamma > \sigma$ and the average citation per post tends towards a constant [57],

$$\lim_{t \rightarrow \infty} m(t) = \frac{\sigma b}{\gamma - \sigma}. \quad (126)$$

By all this, the stationary distribution $Q_n = \lim_{t \rightarrow \infty} P_n(t)$ is a Waring distribution, in the continuous limit a Tsallis–Pareto distribution:

$$Q(x) = \frac{\gamma}{\sigma b} \left(1 + \frac{x}{b}\right)^{-1-\gamma/\sigma}. \quad (127)$$

This distribution scales like

$$Q(x) = \frac{1}{\langle x \rangle} f\left(\frac{x}{\langle x \rangle}\right) \quad (128)$$

with $f(y) \equiv (a + 1) (1 + ay)^{-2-1/a}$ and $a = \sigma/(\gamma - \sigma)$, as the only fit parameter. For a finite $\langle x \rangle = ab$ one needs $a > 0$, i.e. $\gamma > \sigma$. This scaling is demonstrated on various citation and Facebook share data in Fig.5. Technical details of obtaining these data are described in [57], and here in Fig.5 we present an essentially wider survey of various data including scientific citations, Facebook shares and likes and You Tube likes as well.

In closing this subsection we mention that master equations used in another perspective were involved already in the early 1984 for explaining the citation dynamics [58].

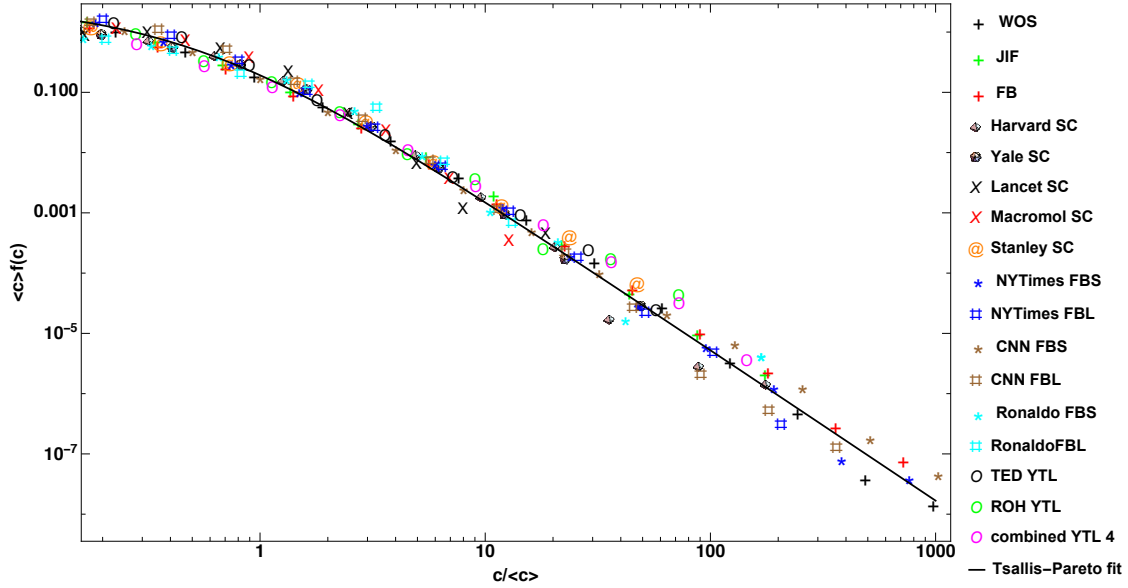


Figure 5: Rescaled distribution of citation numbers, $\langle c \rangle f(c)$, vs the ratio $c/\langle c \rangle$. WOS stands for the Web of Science, FB for the Facebook, JIF for Journal Impact Factor, TED for the Ted Talks channel, and ROH for the Royal Opera House in London. Stanley is a well-known Professor of Physics, Ronaldo a soccer player, and NYTimes abbreviates the newspaper New York Times. Lancet and Macromolecules are scientific journals. Harvard and Yale denote the scientific output of the corresponding universities in a decade. The type of citations are encoded as follows: SC for scientific citations, FBS for Facebook shares, FBL for Facebook likes, and YTL abbreviates you tube likes. The black curve represents the Tsallis-Pareto fit with a single parameter in its scaling form: $a = 2$.

5.3. Hadron production

A simple mechanism will be considered for the hadron production process in high energy heavy-ion and elementary particle collisions. In such collisions a high energy density state is formed, with a huge number of quarks and gluons. It is treated either as an ensemble of partonic jets, inside which a quasi one-dimensional gas of subhadronic partons are present, or a three-dimensional, high temperature strongly coupled quark-gluon plasma. These systems freeze out at the end of a sudden cooling process giving birth to hadrons.

The number of hadrons made, n , is called the multiplicity of a single collision event. In millions of repeated collisions the distribution of this hadron number, the multiplicity distribution, P_n , is evolving during the process. We assume that the measured multiplicity distributions are close to the stationary distribution, Q_n .

For these hadronization processes we construct the following simple model: Having already n hadrons, a new hadron is created with the probability rate μ_n , and a collective re-melting into the prehadron stage happens with the rate γ_n . We conjecture that there is a certain number of newly made hadrons, $\langle n \rangle$, for which the re-melting does not occur. Less hadrons than this number will likely to be created from a zero number state, featuring formally negative γ_n rates for $n < \langle n \rangle$. In this case the yield is proportional to P_n , not with P_0 . More hadrons, $n > \langle n \rangle$, will be re-melted with a positive γ_n rate in this scenario. We work thus with the ansatz $\gamma_n = \sigma(n - \langle n \rangle)$.

Furthermore we assume $\mu_n = \sigma(n/k + 1)\langle n \rangle$, realizing the Matthew principle with linear preference. Certainly, already at $n = 0$, in the state with no hadrons, there is a probability rate to create one, $\mu_0 = \sigma\langle n \rangle$. Already having n hadrons on the other hand helps this process; most of the hadrons to be made are light bosons, mainly pions. The construction of the rates are harmonized for $\gamma_0 + \mu_0 = 0$. For all other n values one has $\gamma_n + \mu_n > 0$.

Accepting all these assumptions, the obtained stationary distribution in our master equation framework is the negative binomial one,

$$Q_n = \binom{n+k-1}{n} \frac{(\langle n \rangle/k)^n}{(1 + \langle n \rangle/k)^{k+n}}. \quad (129)$$

The first moment turns out to be exactly $\langle n \rangle$. This distribution is also generated by the k -th power of the geometrical

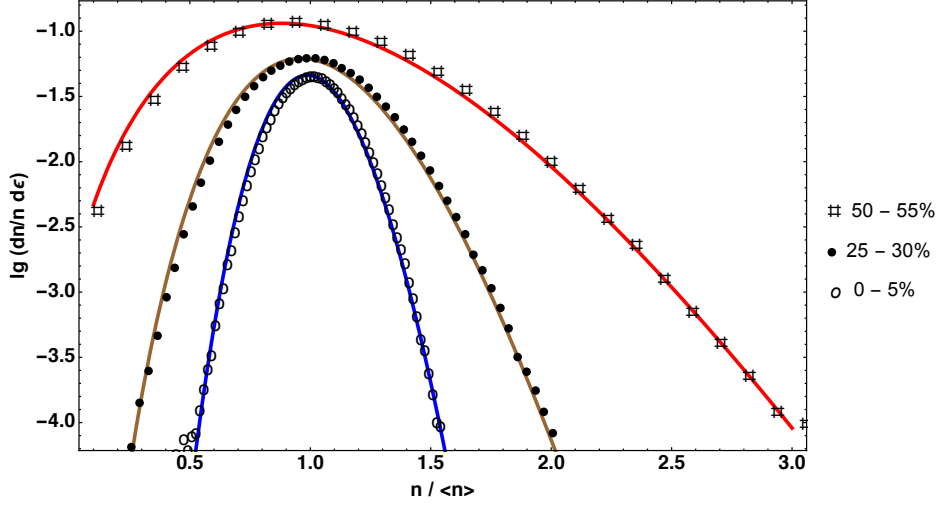


Figure 6: Total charged hadron multiplicity distributions from Au+Au collisions at 200 GeV center of mass energy per incoming nucleon, plotted for different centrality classes: for (a) 0 – 5%, for (b) 25 – 31% and for (c) 55 – 60%, from the bottom to the top. The NBD best fit parameters are as follows: (a) $\langle n \rangle = 61$, $k = 255$; (b) $\langle n \rangle = 27.4$, $k = 50$; (c) $\langle n \rangle = 8.5$, $k = 17$.

series [60],

$$(1-x)^{-k} = \sum_{n=0}^{\infty} \binom{n+k-1}{n} x^n, \quad (130)$$

as a generalization of the binomial formula for negative powers. The second scaled factorial moment,

$$F_2 \equiv \frac{\langle n(n-1) \rangle}{\langle n \rangle^2} = 1 + \frac{1}{k} > 1 \quad (131)$$

indicates that this distribution is super-Poissonian. In the $k \rightarrow \infty$ limit the Poisson distribution emerges when keeping $\langle n \rangle$ finite.

Finally a remark on the negative values of certain γ_n -s: Is it fatal? No, as long as $\mu_n + \gamma_n > 0$, the recursion solution eq.(64) for Q_n works fine. In the above outlined hadronization scenario $\gamma_n + \mu_n = \sigma n(1 + \langle n \rangle / k) > 0$, this condition is fulfilled. The meaning of sometimes positive sometimes negative γ_n resetting rates represents in the state space such a long jump process, which under certain circumstances goes in the opposite direction. However, in this case the dependence on the initial state occupation probability also turns into the same dependence on the final state probability; this is a special, up to now scarcely investigated skew symmetry principle for random processes not satisfying detailed balance condition. Our proof for the decrease of the entropic divergence to the stationary distributions is not directly applicable to this system. We postpone this problem for a future work.

Experimental findings for hadron multiplicity distributions in high energy experiments indeed show results well approximated by the negative binomial (NBD) distribution. A demonstrative example is given by results of the PHENIX experiment at the Relativistic Heavy Ion Collider operating at Brookhaven [61]. Based on publicly available data we have replotted some of the multiplicity distributions for the reaction AuAu at 200 GeV on Fig.6. On the horizontal axis the ratio $n / \langle n \rangle$ is given and on the vertical axis we have the measured normalized jet data, related to the Q_n distributions. The NBD distribution (129) with parameters given in the figure caption offers a fair fit.

The NBD multiplicity distribution also leads to an approximate Tsallis–Pareto distribution in the single particle kinetic energy. Considering the probability of having n particles, P_n , sharing the total energy E we have two, physically different cases, described by mathematically equivalent formulas. In a high-energy jet of partons, moving only in a very narrow cone relative to the leading parton, the phase space is exactly n -dimensional with the total relativistic

kinetic energy (with c being the speed of light):

$$E = c \sum_{j=1}^n |p_j|. \quad (132)$$

At low energy the typical measurement for the hadronic fireball is a two-dimensional transverse momentum distribution. The ensemble of n particles live in a $2n$ -dimensional kinetic phase space, with the total non-relativistic energy for slow particles

$$E = \frac{1}{2m} \sum_{j=1}^{2n} p_j^2. \quad (133)$$

The third dimension is suppressed in the transverse momentum spectra by the narrow rapidity selection.

In both cases the probability density of finding a given energy value, E , is proportional to the occupied phase space volume, $\Omega(E)$. This is the simplest assumption underlying the Boltzmannian statistics. The fixed total energy shell phase space volume can be derived from the volume of the N -ball, constructed according to the kinetic energy formula. One realizes that

$$\Omega_N(E) = \int \delta(E' - E) d\Gamma_N = \frac{1}{dE/dR} \int \delta(R' - R) d\Gamma_N = \frac{1}{dE/dR} \frac{d}{dR} V_N(R) = \frac{d}{dE} V_N(R(E)). \quad (134)$$

The phase-space volume for an N -ball in an L_p norm is given by:

$$V_N^{(p)} \left(\left(\sum_i |x_i|^p \right)^{1/p} \leq R(E) \right) = \frac{\Gamma(1 + 1/p)^N}{\Gamma(1 + N/p)} (2R)^N. \quad (135)$$

The $p = 1$ case with $R(E) = E/c$ describes strongly relativistic jet particles, while the $p = 2$ case with $R(E) = \sqrt{2mE}$ non-relativistic, massive particles. The corresponding hypershell volumes, $\Omega_N^{(p)}(E) = dV_N^{(p)}(E)/dE$, are given as

$$\Omega_n^{(1)}(E) = \frac{d}{dE} \frac{(2E/c)^n}{n!} = \left(\frac{2}{c} \right)^n \frac{E^{n-1}}{(n-1)!}, \quad (136)$$

for the jets with $N = n$ kinetic degrees of freedom and

$$\Omega_{2n}^{(2)}(E) = \frac{d}{dE} \frac{(2m\pi E)^n}{n!} = (2m\pi)^n \frac{E^{n-1}}{(n-1)!} \quad (137)$$

for the massive particles moving in two dimensions with $N = 2n$.

The *single particle energy spectra* reflect the hypershell volume ratio

$$r_{N,g}^{(p)} \equiv \frac{\Omega_g^{(p)}(\epsilon) \Omega_{N-g}^{(p)}(E - \epsilon)}{\Omega_N^{(p)}(E)}, \quad (138)$$

with $g = N/n$ single particle degrees of freedom. This ratio coincides for $N = n$ and $p = 1$ (quasi one-dimensional jet with n particles) with the value at $N = 2n$ with $p = 2$ (two-dimensional non-relativistic gas with $2n$ momentum components):

$$r_{n,1}^{(1)} = r_{2n,2}^{(2)} = \frac{n-1}{E} \left(1 - \frac{\epsilon}{E} \right)^{n-2}. \quad (139)$$

This formula is nonzero only for $n \geq 2$ (the minimum number of particles to share energy is two), and terminates for $\epsilon > E$, which is the maximal energy for the selected particle. We note that by construction

$$\int_0^E r_{N,g}^{(p)}(\epsilon, E) d\epsilon = 1. \quad (140)$$

Obtaining single particle energy spectra from high-energy experiments usually overlays results for different hadron multiplicities, n . Having a probability distribution for the newly produced hadrons, P_n , (please note that also minimum two particles are necessary to initiate a collision), one presents single particle spectra as

$$\frac{1}{\mathcal{N}} \frac{d\mathcal{N}}{d\epsilon} = \sum_{n=2}^{\infty} r_{ng,g}^{(p)}(\epsilon, E) P_{n-2}. \quad (141)$$

The jet and massive two-dimensional gas can be treated with the common formula, eq.(139) here. This also might be the reason why the low-momentum and high-momentum parts of observed p_T -spectra can be covered by a single fit.

Using the negative binomial distribution (129) one obtains

$$\frac{1}{\mathcal{N}} \frac{d\mathcal{N}}{d\epsilon} = \frac{1}{E} \left(1 + \frac{\langle n \rangle}{k} \frac{\epsilon}{E}\right)^{-k-1} \left[1 + \frac{\langle n \rangle}{k} \frac{\epsilon}{E} + \langle n \rangle \left(1 - \frac{\epsilon}{E}\right)\right]. \quad (142)$$

It has a finite value both at $\epsilon = 0$ and at $\epsilon = E$. The latter is due to the fact, that the hypershell volume ratio for making no new hadrons is one, which has to be interpreted as the Heaviside theta function $\Theta(E - \epsilon)$. For small energies, $\epsilon \ll E$, up to a tenth of E , the above result is well-approximated by a Tsallis–Pareto distribution:

$$\frac{1}{\mathcal{N}} \frac{d\mathcal{N}}{d\epsilon} \approx \frac{\langle n \rangle + 1}{E} \left(1 + \frac{\langle n \rangle}{k} \frac{\epsilon}{E}\right)^{-k-1}. \quad (143)$$

Hadronic transverse momentum (p_T) spectra are indeed best fitted by Tsallis–Pareto distributions. Fig.7 shows such experimental findings and different fits, carried out by Gábor Bíró in his MSc thesis at the Eötvös University in 2016. The upper row is for pions, the middle row for kaons and the lower row for protons, particles with different rest mass. Figures in the left column stand for the Boltzmann exponential fit, in the middle column for a pure power-law fit, and finally in the right column for the Tsallis–Pareto fits. The different colored thick curves represent fits to different p_T ranges, as given in the legends. It is obvious that only the Tsallis–Pareto form is able to cover both higher and lower p_T values in the experimental results, while the others fail for the values outside the respective fit ranges [36].

5.4. Income distribution

Another good example is the income distribution in societies. As a general rule one observes in the density function two well distinguishable regimes [62]. One regime is the high income region (usually the upper 2% of the population), where a clear power-law like trend is observable. On the other hand in the low and medium income region (98% of the population) the income distribution can be well fitted by a gamma distribution.

Let us consider the top income region (upper 2 % of the population) first, from the perspective of our model. Here the increase in the income is always a given per cent, not a given amount, so in our master-equation approach a purely linear increase rate will be considered: $\mu(x) = \sigma x$. A constant resetting rate can be assumed by a retirement/death process $\gamma(x) = \gamma$. The above assumptions leads to a power-law tail in the distribution; in fact the original Pareto-law. Such distributions are observed, only in the high-end tail of the income distribution (top 2% of the households) [62]. The Pareto-exponent α obtained in observations is robust. It does not change over decades of years, although the actors in the society and the persons in the top income category are continuously changing [63]. The Pareto exponent, in our model is given as $\alpha = 1 + \gamma/\sigma$, where the σ coefficient in the linear preference law, $\mu(x) = \sigma x$, seemingly follows the resetting rate γ . It is interesting to note here that Pareto’s law has been observed also in historical wealth data. Beginning with ancient societies [64], through classical and medieval ages [65] and also the beginning of capitalism [66]. Income distributions mapped nowadays from more precise, electronically available data confirms it’s generality [63].

For describing the income distributions in the middle and low classes (98% of the society), one has to consider a different choice for the $\gamma(x)$ rates. We will consider the same linear form for the growth rate $\mu(x)$ for persons that are already in the system at a given time moment. Under such an ansatz the resetting rate $\gamma(x)$ is however more complicated. As one reaches a higher income, presumably gets older and thus the resetting rate has to increase as well. This is very different from the very high income region, where we assumed the same resetting rate for all income categories. One also has to take into account that employees that had no income can appear in an income

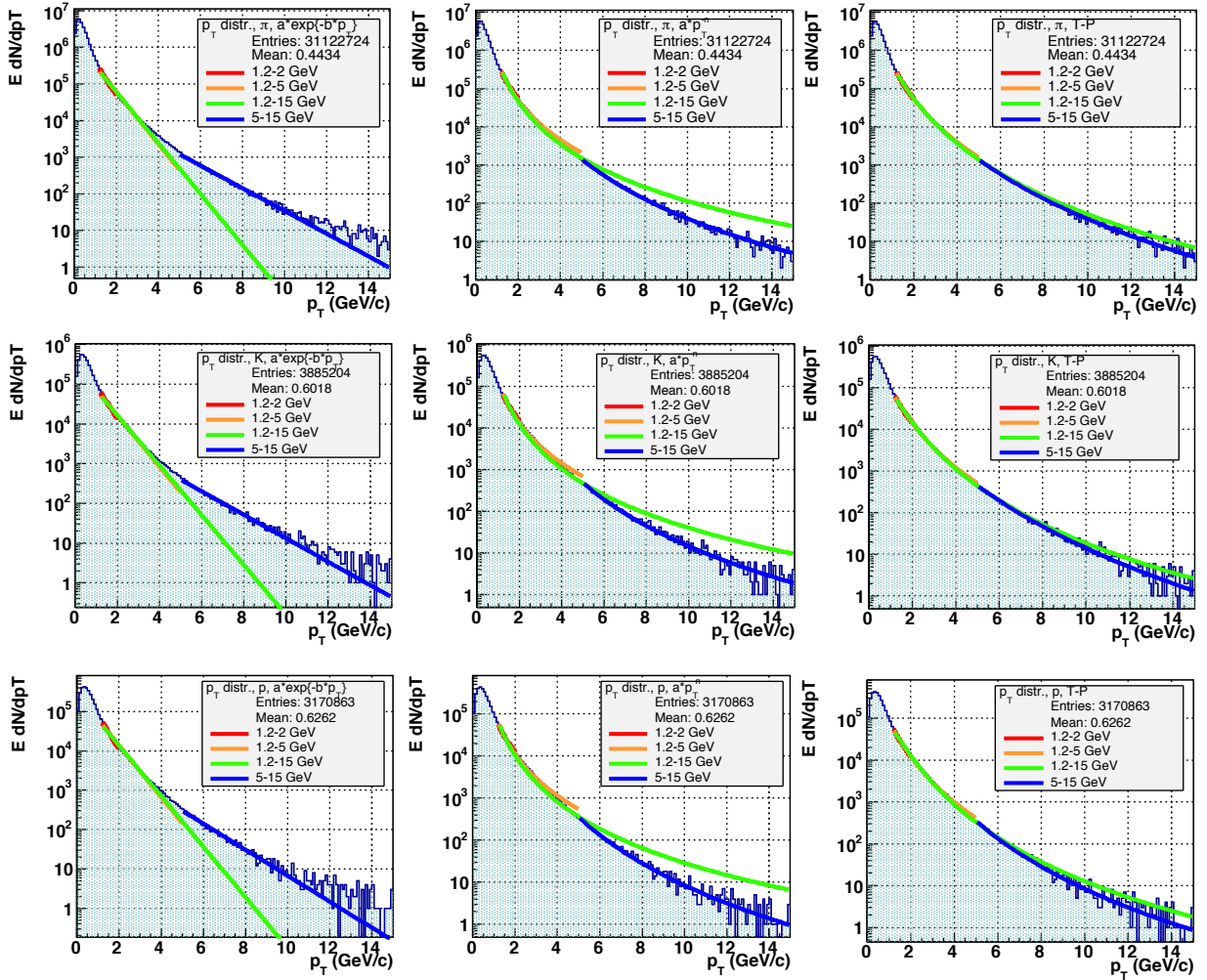


Figure 7: Transverse momentum spectra of different hadrons (pions, kaons and protons from top down) and three different fits to them: exponential (left column), power-law (middle column) and Tsallis-Pareto distributions (right column). Figures from the master thesis of Gábor Bír, with the permission of the author.

category (beginners), but with a bigger probability in the income-categories below the average. We consider thus a smart resetting rate which can become also negative, best balanced at an intermediate income class and increasing with high income. The most simplest linear choice for the γ rates that incorporates all the above discussed effects and which may go also to negative would be $\gamma(x) = \sigma(ax - c)$.

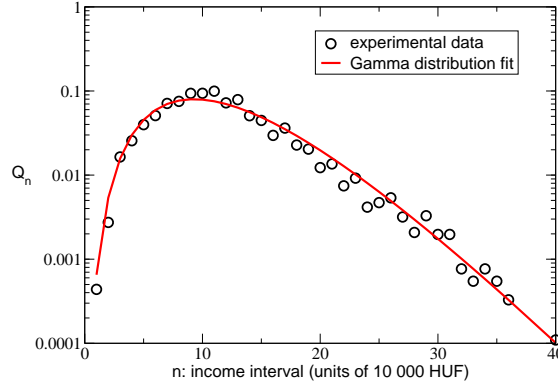


Figure 8: Hungarian income distribution in 2014 according to a non-official survey of KSH in thousand Hungarian Forint units. Dots are binned data and the continuous line is a gamma distribution fit (144) with $c = 4.6$ and $a = 0.3883$

The above assumptions lead to a gamma distribution at stationarity:

$$Q(x) = \frac{a^c}{\Gamma(c)} x^{c-1} e^{-ax}. \quad (144)$$

Here $\Gamma(c)$ denotes Euler's gamma function with the property $\Gamma(c + 1) = c\Gamma(c)$. Certainly, this $\gamma(x)$ is also negative for $x < c/a = \langle x \rangle$.

As a demonstration we present the result of a partial net income survey made by the Central Statistics Bureau (KSH) in Hungary in 2014. The data sample, binned by 10,000 HUF bins, is nicely approximated by a gamma distribution with $c = 4.6$ and $a = 0.3883$, resulting in the average income of $\langle x \rangle = c/a = 118,465$ HUF. The maximum of the fitted curve is at $x_m = (c - 1)/a = 92,711$ HUF, this was the net income most people had.

5.5. Biodiversity

A major challenge in ecology is to understand the abundance distribution in communities of neutral species [67]. Given an ensemble of species which do not compete with each other, except sharing a common ecological niche, the abundance distribution describes the PDF, Q_n , for having n individuals in one of the species.

The most popular and well-know fit to the observed distribution used by ecologists is the famous Fisher's log series which suggests for the number of species with n individuals the value [68]:

$$S_n = \alpha \frac{a^n}{n} \quad (145)$$

where α and a can be determined knowing the total number of individuals,

$$N \equiv \sum_{n=1}^{\infty} nS_n = \alpha \frac{a}{1-a}, \quad (146)$$

and the number of species in the studied territory,

$$S \equiv \sum_{n=1}^{\infty} S_n = -\alpha \ln(1-a). \quad (147)$$

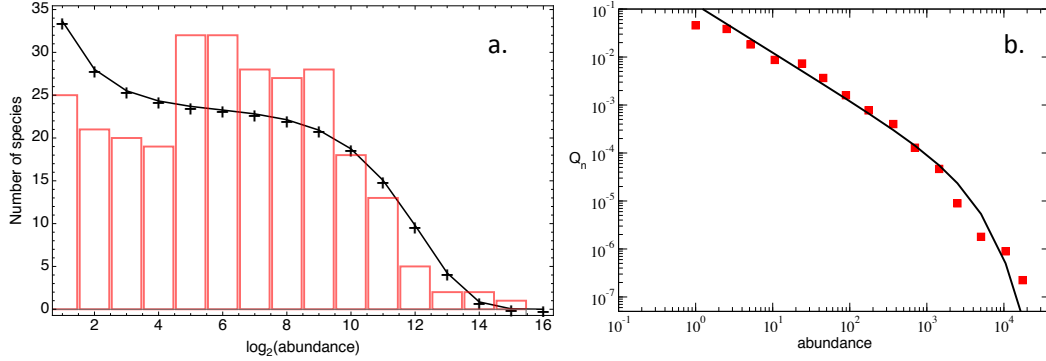


Figure 9: Tree species abundance distribution for the 1995 BCI data. Fig. a presents the Pearson plot (W_k with $k = \log_2 n$), Fig. b the PDF (Q_n). Continuous lines in both parts stand for the Fisher log series fits.

This leads to

$$S = \alpha \ln \left(1 + \frac{N}{\alpha} \right) \quad \text{with} \quad a = \frac{N}{\alpha + N}. \quad (148)$$

Nowadays exhaustive data sets are available for tree communities on large territories. One of the most known is the Barro Colorado Island Tropical Tree Census (BCI) [69], administrated by the Smithsonian Tropical Research Institute in the U.S. In this census more than 240,000 stems and over 300 tree and shrub species are accurately mapped. Data are publicly available on request [69].

As an example for the appropriateness of the Fisher log series fit [70], on Fig.9 we present abundance distribution from the BCI Tropical Tree Census in 1995 determined from a 25 ha territory containing $N = 112543$ trees belonging to a total number of $S = 273$ species. Two different plots are shown. One is the Preston-type plot (Figure a.), where we plot the number of species found in abundance intervals of consecutively doubling lengths. Prestons method of plotting is motivated by the fact that abundances can vary over several orders of magnitude and there are far fewer abundant species than rare ones. Using fixed-length abundance intervals would result in large statistical fluctuations at the tail of the curve. In Fig.9a we indicated by bars the number of species found in such increasing abundance intervals and with black symbols the number predicted by the Fishers log-series distribution:

$$W_k = \sum_{n=2^k}^{2^{k+1}-1} S_n. \quad (149)$$

Please note that the value of α and a are not fitted, they are computed from the values of S and N based on equations (148). In the second plot (Figure b.) we have shown the PDF of the distribution, i.e. $Q_n = S_n/S$ computed from the BCI data and the one calculated from equation (145).

The log series abundance distributions can easily be reproduced in the framework of our model, offering a possible explanation for the mechanism behind forming such a distribution. Let us assume a growth phenomena with resetting, and start from an empty territory. We assume a pure linear preference rate for the local growth factor, $\mu_n = \sigma n$. Then apply the recursion rule for the stationary distribution (64) using the log series prediction given eq.(145). We obtain

$$\sigma(n-1) \alpha \frac{a^{n-1}}{n-1} = (\sigma n + \gamma_n) \alpha \frac{a^n}{n}. \quad (150)$$

The solution for the resetting rate, γ_n , is also linear:

$$\gamma_n = n\sigma \left(\frac{1}{a} - 1 \right). \quad (151)$$

Since $a < 1$ for Q_n being normalizable, this reset rate is always positive. We interpret it as a rate of a total destruction of all individuals in the species, as an extinction rate (describing the frequency of long jumps from n to zero in a

short time step). Its linear dependence on the number n suggests that the extinction rate, increases with the size of the species suggesting that larger species are more vulnerable.

The approach presented here is on the mean field level without caring for spatiality. More advanced models also consider the distribution of the individuals and species in space and their correlations [71].

5.6. Settlement size distribution

A further interesting application field is the study of settlement size distribution. Data from different countries (US, France, Japan, China, India) follow similar trends. Most fits show a log-normal distribution around the maximum frequency (middle sized cities), and at the same time a high-end distribution tail following Pareto's law [72]. We illustrate this trend for the settlement size distribution in Hungary. On the left panel of Figure 10 we show the density function for the settlement-size distribution of all 3154 settlements in Hungary. The black dots represent the computed density function using a logarithmic binning method. The blue curve shows a log-normal fit

$$\rho(x) = \frac{1}{x\sigma\sqrt{2\pi}} \exp\left(-\frac{(\ln(x) - m)^2}{2\sigma^2}\right) \quad (152)$$

with $\sigma = 1.2$ and $m = 6.7$. The red curves illustrate a power-law trend $\rho(x) \propto x^\alpha$ with $\alpha = -2$. The above observations turn our attention to the possibility that for large settlements a different dynamics is realized than for small and middle sized ones. This is somehow similar with the case discussed in the subsection devoted to the income distribution. In order to elaborate on this guess, we use again the framework of our model and take a different approach now. Having data on $Q(x)$ and assuming a certain expression for the local rate, $\mu(x)$, we can express the nonlocal rate, $\gamma(x)$, based on the stationary solution to the evolution equation (77). In such a view one can determine the unknown model parameters necessary for reproducing the observed distributions. More specifically, the unknown $\gamma(x)$ will be given by the continuous version of eq.(64):

$$\gamma(x) = -\frac{1}{Q(x)} \frac{\partial}{\partial x} (\mu(x)Q(x)). \quad (153)$$

This result allows also negative values for $\gamma(x)$. These can be interpreted as nonlocal transition rates from the ground state directly to a finite x size. This situation reminds us to the situation encountered in the discussion of income distribution and particle multiplicities in high energy experiments.

Considering in particular a linear preference rate in the local growth rate, $\mu(x) = \sigma x$, we obtain

$$\frac{1}{\sigma} \gamma(x) = -1 - \frac{\partial \ln Q(x)}{\partial \ln x}. \quad (154)$$

In particular for a power-law tail, $Q(x) \sim x^{-\alpha}$ one obtains a constant nonlocal rate, $\gamma(x) = \sigma(-1 + \alpha)$. It is positive for $\alpha > 1$, which at the same time is the condition for the normalizability of $Q(x)$. The log-normal distribution on the other hand,

$$Q(x) \sim \frac{1}{x} \exp\left[-\frac{a}{2} \ln^2\left(\frac{x}{b}\right)\right], \quad (155)$$

assumes:

$$\gamma(x) = a \ln \frac{x}{b}. \quad (156)$$

To illustrate the picture outlined above, in the right panel of Fig.10 we show the value of $\gamma(x)$ numerically derived from equation (154) plotted on normal-log scale. Indeed the shape of $\gamma(x)$ on the normal-log scale justify both assumptions: a linear rise at small and middle sized settlements and a saturation to a constant value at large sizes. One can observe on this picture that the transition between the two regimes correspond to the one sketched in the left panel of Fig. 10, namely the region where a log-normal fit is appropriate and the region where the power-law trend is observable.

If one accepts the assumptions inherent in the unidirectional growth and reset model, the $\gamma(x)$ versus $\ln x$ plot in this case helps to distinguish distribution models more efficiently than the familiar $Q(x)$ or cumulated plots. The data presented for Hungary is in agreement with findings in other countries (US [73], India [74], China [75], OECD countries [76]).

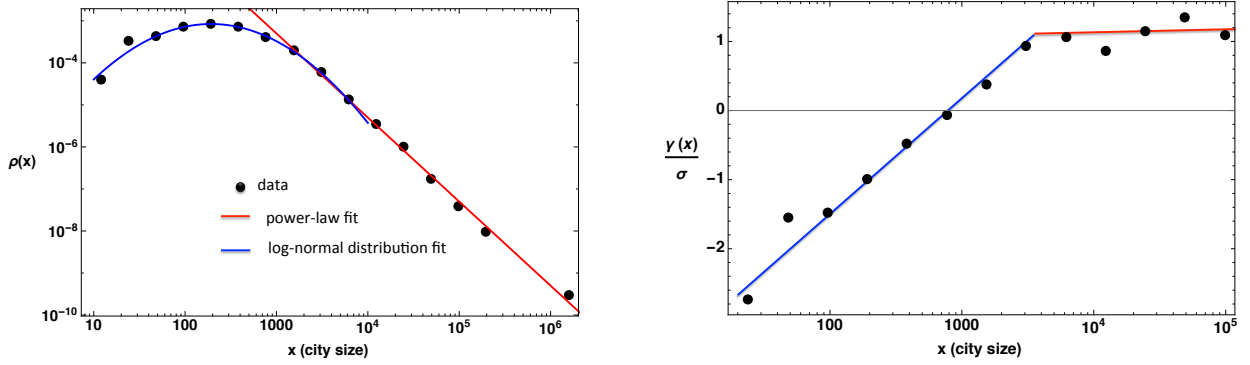


Figure 10: (Left panel) Density function for the Hungarian settlement population size distribution on a log-log plot. The log-binned data is presented by black dots, the power-law trend with exponent $\alpha = -2$ is illustrated by the red line, the log-normal fit to the small and middle size settlement region is illustrated by the blue line ($\sigma = 1.2$ and $m = 6.7$). (Right panel) The $\gamma(x)/\sigma$ value numerically derived from equation (154).

6. Conclusion

In conclusion we have reviewed a model for unidirectional growth augmented by rare resets to the ground state with great potential of applications to complex systems. We have considered fundamental questions, and presented a new result about the stability of stationary PDF-s. The proof is based on a careful analysis of the notion of entropic divergence (by some called entropic distance, although its definition is usually not symmetric in the two distributions as arguments). We have found that for a global approach towards the stationary PDF, as far as it exists, in all linear and nonlinear master equation approaches *it is sufficient* that the definition of entropic divergence is based on a core function with definite convexity. This property holds for any positive transition rate from the state $|m\rangle$ to $|n\rangle$ in general as long as the PDF dependent factor in all terms involves the initial state of the microtransition only, in form of a general positive function, $a(P_m)$. Then we investigated factorizing dependencies on the initial and final state occupation probabilities in such microtransitions, $w_{nm}a(P_m)b(P_n)$. We have found that only rates satisfying the *detailed balance* condition ensure the steady decrease of the entropic divergence to the stationary PDF.

During this proof a surprising consequence arose. Using the traditional kernel function for defining the entropic divergence, $\sigma(\xi) = -\ln \xi$, in case of a nonlinear power dependence on the initial state occupation in the elementary transitions, $a(P_m) \sim P_m^q$, the resulting entropic divergence to the stationary PDF becomes non-Boltzmannian. This result is a beautiful generalization of the Kullback–Leibler entropic divergence. Moreover, seeking a relative entropy interpretation for this result, one realizes that the entropic divergence from the uniform distribution to the stationary PDF is proportional to the difference of Tsallis–entropies, and not to the Rényi ones (cf. eqs.(43,44)).

Beyond these general investigations we have concentrated to a particular class of stochastic models, describing unidirectional growth and resetting processes. This simple approach reduces the possible micro-transitions to a local one, from $|n\rangle$ to $|n+1\rangle$ with the rate μ_n , and assumes a resetting from any state $|n\rangle$ to the ground state $|0\rangle$ with a rate γ_n . In spite the compactness and austerity of its formulation (only with two dynamical concepts) this model performs surprisingly abundant. First, it helps to understand theoretical questions: i) the emergence of stationary distributions and a soliton-like approach to them, ii) the validity of a formula between the elementary local and nonlocal rates through the stationary distribution, reminding very much to the fluctuation–dissipation theorem, iii) the continuous limit of discrete step-like processes ($n \rightarrow x$), and iv) the reproduction of a number of well known and widely used distributions as stationary PDF-s based on simple assumptions on the rates $\mu(x)$ and $\gamma(x)$. Our presentation offers a straightforward alternative to the historical derivations. Second, it proves to be useful for a long list of applications: i) complex network degree distributions, ii) citation distribution of scientific papers and Facebook post shares, iii) hadron production in high energy experiments, iv) income and wealth distribution, v) biodiversity vi) city size distribution, and possibly further statistical phenomena, not discussed here.

In most applications a linear preference was assumed in the local growth rate, $\mu(x) \sim x$, and a constancy in the resetting rate, $\gamma(x) = \gamma$, with a few notable exceptions. From the linear local rate – constant resetting rate dynamics a

Tsallis–Pareto PDF emerges. In the case when both type of rates are constant, the stationary PDF is exponential, and finally with the resetting rate growing as the logarithm, $\gamma(x) \sim \ln x$, and the local growth rate linearly, a log-normal distribution is established. Certainly, further stationary distributions can belong to various different assumptions about these rates. We would like to call the attention also to the reverse method: having information about the final distribution, $Q(x)$, and one of the rates, the other one can be obtained by the statistical fluctuation–dissipation relation. This opens a novel view to the analysis and interpretation of numerical statistical data, much akin to the hazard rate and cumulative hazard analysis in life expectancy and fatigue studies. For non-constant $\gamma(x)$ we hence have generalized the concept of cumulative hazard and hazard rate.

This somewhat longer paper is not intended to be a review in the classical sense. The emphasis was put on unfolding of a simple original idea, investigating the consequences and application possibilities of unidirectional growth and resetting. We did not have the occasion to exhaustively cite and review many important works on theory or applications on complex systems with random dynamics. Concerning our contributions, we did not limit ourselves to a simple repetition of earlier published results. Several new ideas both in theoretical derivations and real world applications are presented here in this new context.

Closing this paper we outline some possible further research directions on the main topic treated here, based on unresolved questions. In the theory of investigating the stability of stationary PDF-s and the possible generalized formulas for entropy and entropic divergence further master equation classes have to be investigated more closely. In particular local and nonlocal transition rates should be considered together without a restriction to one direction (growth only) and without selecting out only a single state ($n = 0$) as a special one. Also the interpretation of negative γ_n values remained incomplete. Finally, a much greater number of application on real world data shall be undertaken in the future. In particular it would be instructive to gather complementary knowledge about the micro-transition rates (μ_n, γ_n, w_{nm}) and not only to fit the PDF-s.

Acknowledgment

T. S. B. thanks the University Babeş-Bolyai in Cluj for the UBB Star Fellowship. Discussions with András Telcs, Levente Varga, Hawong Jeong, Géza Tóth and Mounir Afifi are hereby acknowledged. We thank Constantino Tsallis for encouraging to present a review sized publication about the achievements of our simple model. This work has been partially supported by the Hungarian National Bureau for Research, Innovation and Development (NKFIH) under project Nr. K 123815 and by the Romanian Research Council UEFSCDI, PN-III-P4-PCE-2016-0363.

References

- [1] E. Ising, *Beitrag zur Theorie des Ferromagnetismus*, Z. Phys. **31** (1925) 253.
- [2] P. Erdos, A. Renyi, *On random graphs*, Publicationes Mathematicae **6** (1959) 290.
- [3] E. N. Gilbert, *Random graphs*, Ann. Math. Statistics **30** (1959) 1141.
- [4] L. D. Landau, *On the theory of phase transitions*, Zh. Exp. Theor. Fiz. **7** (1937) 19.
- [5] R. Manke, J. Kapuzs, I. Lubashevsky, *Physics of Stochastic Processes*, Chap.3, Wiley & Sons, 2009.
- [6] B. Corominas-Murtra, R. Hanel, S. Thurner, *Sample space reducing cascading processes produce the full spectrum of scaling exponents*, Scientific Reports **7**, 11223 (2017)
- [7] S. Kullback, R. A. Leibler, *On information and sufficiency*, Ann. Math. Statistics **22** (1951) 79.
- [8] C. Tsallis, *Possible generalization of Boltzmann–Gibbs statistics*, J. Stat. Phys. **52** (1988) 479.
- [9] J. Havrda, F. Charvát, *Quantification method of classification processes. Concept of structural α -entropy*, Kybernetika **3** (1967) 1359.
- [10] J. Aczél, Z. Daróczy, *On Measures of Information and Their Characterizations*, Academic Press, New York, 1975.
- [11] M. D. Esteban, D. Morales, *A Summary on Entropy Statistics*, Kybernetika **31** (1995) 337.
- [12] I. Csiszár, *Axiomatic Characterizations of Information Measures*, Entropy **10** (2008) 261.
- [13] E. M. F. Curado, F. D. Nobre, *Derivation of nonlinear Fokker-Planck equations by means of approximations to the master equation*, Phys. Rev. E **67** (2003) 021107.
- [14] F. D. Nobre, E. M. F. Curado, G. Rowlands, *A procedure for obtaining general nonlinear Fokker-Planck equations*, Physica A **334** (2004) 109.
- [15] V. Schwämmle, F. D. Nobre, E. M. F. Curado, *Consequences of the H theorem from nonlinear Fokker-Planck equations*, Phys. Rev. E **76** (2007) 041123.
- [16] C. M. Vieira, H. A. Carmona, J. S. Andrade Jr., A. A. Moreira, *General continuum approach for dissipative systems of repulsive particles*, Phys. Rev. E **93** (2016) 060103(R).
- [17] A. M. C. Souza, R. F. S. Andrade, F. D. Nobre, E. M. F. Curado, *Thermodynamic Framework for Compact q -Gaussian Distributions*, Physica A **491** (2018) 153.

- [18] E. M. F. Curado, A. M. C. Souza, F. D. Nobre, R. F. S. Andrade, *Carnot cycle for interacting particles in the absence of thermal noise*, Phys. Rev. E **89** (2014) 022117.
- [19] F. D. Nobre, E. M. F. Curado, A. M. C. Souza, R. F. S. Andrade, *Consistent thermodynamic framework for interacting particles by neglecting thermal noise*, Phys. Rev. E **91** (2015) 022135.
- [20] M. S. Ribeiro, G. A. Casas, F. D. Nobre, *Second law and entropy production in a nonextensive system*, Phys. Rev. E **91** (2015) 012140.
- [21] Bible, Matthew 13:12, King James version.
- [22] J. S. Andrade Jr., G. F. T. da Silva, A. A. Moreira, F. D. Nobre, E. M. F. Curado, *Thermostatistics of Overdamped Motion of Interacting Particles*, Phys. Rev. Lett. **105** (2010) 260601.
- [23] M. S. Ribeiro, F. D. Nobre, E. M. F. Curado, *Time evolution of interacting vortices under overdamped motion*, Phys. Rev. E **85** (2012) 021146.
- [24] T. Biró, Z. Nédá, *Dynamical Stationarity as a Result of Sustained Random Growth*, Phys. Rev. E **95** (2017) 032130.
- [25] A. Einstein, *Die von molekularkinetischen Theorie der Wärme geforderte Bewegung von in ruhenden Flüssigkeiten suspendierten Teilchen*, Ann. Phys. **18** (1905) 549.
- [26] J. Crank, *The Mathematics of Diffusion*, Oxford, Clarendon Press, 1956.
- [27] J. Philibert, *One and half century of diffusion: beyond Fick and Einstein*, Diffusion Fundamentals **2** (2005) 1.1 - 1.10
- [28] H. Rishken, T. Frank, *The Fokker-Planck Equation*, Springer, Series in Synergetics, (1996).
- [29] J. O. Irwin: *The Place of Mathematics in Medical and Biological Statistics* J. Roy. Stat. Soc. A **126** (1963) 1-45
- [30] J. O. Irwin: *The Generalized Waring Distribution Applied to Accident Theory* J. Roy. Stat. Soc. A **131** (1968) 205-225
- [31] G. K. Zipf, *Human Behavior and Principle of Least Effort* (Addison-Wesley, Cambridge, MA, 1949).
- [32] B. Gompertz, *On the nature of the function expressive of the law of human mortality and on the new mode of determining the value of life contingencies*, Phil. Trans. R. Soc. A **115** (1825) 513-580.
- [33] L. Benkhelifa, *The beta generalized Gompertz distribution*, App. Math. Modeling (online) (2017) 1-18.
- [34] Chin-Diew Lai, Min Xie, *Stochastic Ageing and Dependence for Reliability*, Springer 2006.
- [35] E. Xekalaki, *Hazard functions and life distributions in discrete time*, Comm. Statistics **12** (1983) 2503.
- [36] G. Biró, *The application of the new generation of detector simulations in high energy physics for the investigation of identified hadron spectra*, MSc thesis, 2016, Eotvos University, Budapest http://birogabesz.web.elte.hu/MSc_Diplomamunka/
- [37] T. S. Biró, A. Jakovác, *Power-law tails from multiplicative noise*, Phys. Rev. Lett. **94** (2005), 132302
- [38] T. S. Biró, G. Györgyi, A. Jakovác, G. Purcsel, *Non-Gibbs Particle Spectra from Thermal Equilibrium*, arXiv:hep-ph/0409157, Never published in a refereed journal.
- [39] T. S. Biró, G. Györgyi, A. Jakovác, G. Purcsel, *A non-conventional description of Quark Matter*, J. Phys. G **31** (2005) S759.
- [40] T. S. Biró, G. Purcsel, G. Györgyi, A. Jakovác, Zs. Schram, *Power-law tailed spectra from equilibrium*, Nucl. Phys. A **774** (2006) 845.
- [41] B. Corominas-Murtra, R. Hanel, L. Zavoian, S. Thurner, *How noise determines the statistics of simple path dependent systems*, arXiv:1706.10202
- [42] A. L. Barabasi, R. Albert, *Emergence of scaling in random networks*, Science **286** (1999) 509.
- [43] R. Albert, A. L. Barabási, *Statistical mechanics of complex networks*, Rev. Mod. Phys. **74** (2002) 47.
- [44] W. Deng, W. Lee, X. Cai, Q. A. Wang, *The exponential degree distribution in complex networks: Non-equilibrium network theory, numerical simulation and empirical data*, Physica A **390** (2011) 1481.
- [45] L. Kullmann, J. Kertesz, Kullman, *Preferential growth: exact solution of the time dependent distributions*, Phys. Rev. E **63** (2001) 051112.
- [46] R. Albert, H. Yeong, A. L. Barabási, *Error and attack tolerance of complex networks*, Nature **406** (2000) 378.
- [47] S. Thurner, F. Kyriakopoulos, C. Tsallis, Phys. Rev. E **76** (2007) 036111.
- [48] H. Yeong, Z. Nédá, A. L. Barabási, *Measuring preferential attachment in evolving networks*, Eur. Phys. Lett. **61** (2003) 567.
- [49] A. Derzsi, N. Derzsy, E. Káptalan, Z. Nédá, *Topology of the ERASMUS student mobility network*, Physica A **390** (2011) 2601.
- [50] Hungarian talent supporting organizations network <http://tehetseg.hu/en/programmes>
- [51] Z. Nédá: Educational networks (presentation given at the International Conference and European Talent Day, 2014, May 8-10, 2014, Budapest, Hungary)
- [52] M. Afifi, *Scaling in the space-time of the Internet* (Master dissertation in Computational Physics, Babes-Bolyai University, Cluj, Romania, 2017, supervisor: Z. Nédá)
- [53] The CAIDA UCSD IPv4 Routed /24 Topology Dataset - May, 2017 https://www.caida.org/data/active/ipv4_routed_24_topology_dataset.xml
- [54] P. L. Krapivsky, S. Redner, F. Leyvraz, *Connecting of Growing Random Networks*, Phys. Rev. Lett. **85** (2000) 4629.
- [55] P. L. Krapivsky, G. J. Rodgers, S. Redner, *Degree Distributions of Growing Networks*, Phys. Rev. Lett. **86** (2001) 5401.
- [56] S. N. Dorogovtsev, J. F. F. Mendes, *Evolution of networks with aging of sites*, Phys. Rev. E **62** (2000) 1842.
- [57] Z. Nédá, L. Varga, T. S. Biró, *Science and Facebook: the same popularity law!* Plos One **12** (2017) e0179656.
- [58] A. Schubert, W. Glänzel, *A dynamic look at a class of skew distributions. A model with scientometric applications*, Scientometrics **6** (1984) 149.
- [59] T. Osada, N. Nakajima, M. Biyajima, N. Suzuki, *Analyses of multiplicity distributions by means of the Modified Negative Binomial Distribution and its KNO scaling function* Prog. Theor. Phys. **98**, 1289 (1997).
- [60] M. Biyajima, N. Suzuki, G. Wilk, Z. Włodarczyk, *Totally chaotic Poisson-like Sources in Multiparticle Production Processes?* Phys. Lett. B **386** (1996) 297.
- [61] Adare et al., PHENIX Collaboration, Phys. Rev. C **78** (2008) 044902.
- [62] V. N. Yakovenko, J. B. Rosser Jr., *Statistical mechanics of money, wealth and income*, Rev. Mod. Phys. **81** (2009) 1703.
- [63] N. Derzsy, Z. Nédá, M. A. Santos, *Income distribution patterns from a complete social security data base*, Physica A **391** (2012) 5611.
- [64] A. Y. Abul-Magd, *Wealth distribution in an ancient Egyptian society*, Phys. Rev. E **66** (2002) 057104.
- [65] G. Hegyi, Z. Nédá, M. A. Santos, *Wealth distribution and Pareto's law in the HUNGARIAN medieval society*, Physica A **380** (2007) 271.
- [66] V. Pareto, *Cours d'économie politique*, vol.2, Macmillian, Paris 1897.
- [67] S. P. Hubbell, *The unified neutral theory of biodiversity and biogeography*, Princeton University Press, Princeton, 2001.

- [68] R. A. Fisher, A. S. Corbet, C. B. Williams, *The relation between the number of species and the number of individuals in a random sample of an animal population*, J. Anim. Ecol. **12** (1943) 42.
- [69] R. Condit, *Tropical Forest Census Plots: Methods and Results from Barrow Colorado Island*, Springer, Berlin, 1998.
- [70] S. Horvát, A. Derzsi, Z. Nédá, A. Balog, *A spatially explicit model for tropical tree diversity patterns*, J. Theor. Biol. **265** (2010) 517.
- [71] A. Derzsi, Z. Nédá, *A seed diffusion model for tropical tree diversity patterns*, Physica A **391** (2012) 4798.
- [72] E.H. Decker, A.J. Kerkhoff and M.E. Moses, *Global Patterns of City Size Distributions and Their Fundamental Drivers*, Plos One **2** (2007) e934.
- [73] J. Luckstead, D. Devadoss, *Pareto tails and lognormal body of US cities size distribution*, Physica A **465** (2017) 573.
- [74] J. Luckstead, S. Devadoss, D. Danforth, *The size distributions of all Indian cities*, Physica A **474** (2017) 237.
- [75] J. Luckstead, D. Devadoss, *A comparison of city size distributions for China and India from 1950 to 2010*, Economic Letters **124** (2014) 290.
- [76] P. Veneri, *On City Size Distribution: Evidence from OECD Functional Urban Areas*, OECD Regional Development Working Papers , 2013/27, OECD Publishing, Paris. <http://dx.doi.org/10.1787/5k3tt100wf7j-en>